THE APPLICATION OF DESCRIBING FUNCTION THEORY TO RAMP INPUTS AND DISSYMMETRIC NONLINEARITIES

DONALD A. MILLER
and
ROGER H. KATTMANN

THE APPLICATION OF DESCRIBING FUNCTION THEORY TO RAMP INPUTS AND DISSYMMETRIC NONLINEARITIES

* * * * *

Donald A. Miller

and

Roger H. Kattmann

THE APPLICATION OF DESCRIBING FUNCTION THEORY TO RAMP INPUTS AND DISSYMMETRIC NONLINEARITIES

by

Donald A. Miller

Lieutenant Commander, United States Navy

and

Roger H. Kattmann

Lieutenant, United States Navy

Submitted in partial fulfillment of
the requirements for the degree of

MASTER OF SCIENCE

IN

ELECTRICAL ENGINEERING

United States Naval Postgraduate School
Monterey, California

1962

THE APPLICATION OF DESCRIBING FUNCTION THEORY TO RAMP INPUTS AND DISSYMMETRIC NONLINEARITIES

by

Donald A. Miller

and

Roger H. Kattmann

This work is accepted as fulfilling
the thesis requirements for the degree of
MASTER OF SCIENCE
IN
ELECTRICAL ENGINEERING
from the
United States Naval Postgraduate School

A generalized describing function is derived for a dissymmetric relay with D. C. components in both the input and output paths. Methods of evaluating the D. C. components are discussed. The describing function is applied to the analysis of step and disturbance inputs.

The describing function is modified to allow computation of the D. C. and sinusoidal components of the error signal when a ramp input is applied. The applicability of the method in various situations is discussed.

The validity of the describing function analysis was investigated by comparing calculated responses with actual system response, as simulated on the analog computer.

The authors wish to express their appreciation for the invaluable counsel and perceptive suggestions provided by Professor G. J. Thaler as faculty advisor for this project.

TABLE OF CONTENTS

LIST OF ILLUSTRATIONS

LIST OF ILLUSTRATIONS

LIST OF ILLUSTRATIONS

LIST OF TABLES

LIST OF SYMBOLS AND ABBREVIATIONS

Symbol	Description
Θ_i	input command signal of a servomechanism
Θ_o	output position of a servomechanism
$\mathcal{E}$	servo system error signal
$\overline{\mathcal{E}}$	Laplace transform of $\mathcal{E}$
I(t)	input signal to non-linear element
W	d.c. component of I(t)
X	amplitude of sinusoidal component of I(t)
ω	frequency of sinusoidal component of I(t)
O(t)	output signal from non-linear element
$\frac{a_o}{2}$	d.c. component of O(t)
a_1	coefficient of $\cos \omega t$ in Fourier series expansion of O(t)
b_1	coefficient of $\sin \omega t$ in Fourier series expansion of O(t)
G_d	generalized describing function for a non-linear element
G_{dn}	non-dimensionalized ramp describing function
ϕ	phase shift associated with G_d or G_{dn}
s	the Laplace variable
$\pi_i(s + p_i)$	product of factors of the form (s + p)
G(s), $G_1(s)$, $G_2(s)$	Laplace transforms of linear elements in a servomechanism
u(t)	the unit step function
k	transient response gain of a linear element

LIST OF SYMBOLS AND ABBREVIATIONS

Symbol	Description
k_v	frequency response gain of a linear element
Y_n	relay output voltage
p_n	relay pull-in voltage
d_n	relay drop-out voltage
α_n	relay pull-in angle
β_n	relay drop-out angle
	note: in the preceding five symbols, n = 1 for the positive side of the relay, and n = 2 for the negative side.
R_p	$\frac{p_1 + p_2}{2X}$
R_d	$\frac{d_1 + d_2}{2X}$
Z	$\frac{X}{p_1 - d_1}$
D_h	$\frac{p_1 + p_2}{p_1 - d_1}$
c	subscript denoting a critical value of X, Z, or D_h at which the system changes from one mode of operation to another.

CHAPTER I

INTRODUCTION

In recent years, the describing function method has been widely used in the analysis of servomechanisms containing non-linear elements (1). The basic describing function technique consists of "linearizing" the non-linear portion of the system by assuming that:

1. The input to the non-linear device is a pure sine wave of known amplitude.
2. The higher harmonics in the output of the non-linear device may be neglected.

A representative describing function is then calculated by computing the amplitude gain and phase shift between the input and the fundamental frequency of the fourier series expansion of the output wave. These techniques are thoroughly discussed in standard texts (2).

In some systems, however, the presence of the non-linearity may cause a D. C. component to exist in either the input or output path, or both. This is particularly true with dissymmetric non-linearities (3). A similar situation can be caused in many symmetric systems by introducing a ramp input. In either case, the D. C. component may cause a change in the magnitude and/or phase of the fundamental frequency of the output from the non-linear element, and it may result in a significant change in the stability characteristics of the system.

It is therefore advantageous to define a generalized describing function, based on the following assumptions:

1. The input to the non-linear element is a pure sine wave superimposed on a pure D. C. component.

2. The higher harmonics in the output of the non-linear element may be neglected. In this case, the output of the non-linear element may be reduced to a pure sine wave superimposed on a pure D. C. component, where both terms may be evaluated from the fourier series expansion of the output wave.

The generalized describing function still consists of the amplitude gain and phase shift between the sinusoidal component of the input and the fundamental frequency component of the output wave.

The purpose of this report is to develop the generalized describing function for a dissymmetric relay and to investigate the characteristics of servomechanisms containing such elements. The report includes a discussion of methods of determining the magnitudes of the D. C. components; an analysis of system stability for step or disturbance inputs; and an analysis and discussion of the system response to step and ramp inputs.

CHAPTER II

DETERMINATION OF D. C. SIGNAL LEVELS

2.1 General Considerations

In all cases investigated in this report, it will be assumed that the block diagram of the servomechanism can be reduced to the form shown in figure 2.1, where $G_1(s)$ and $G_2(s)$ represent the linear portions of a type 1 servomechanism, and G_d is the linearized describing function which represents the non-linear element in the system.

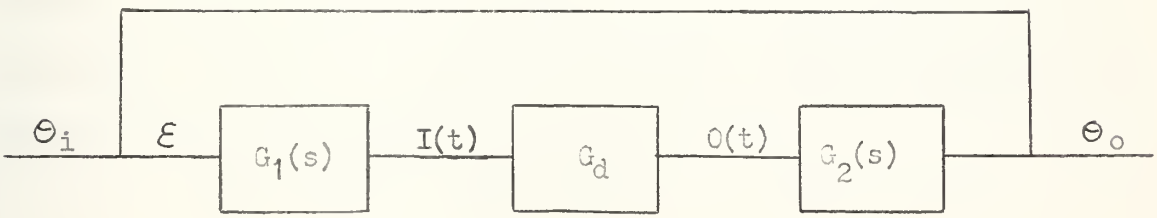

Figure 2.1 Block diagram of a servomechanism containing a dissymmetric non-linearity.

In addition, it will be assumed that the servo loop acts sufficiently like a low pass filter so that only the first harmonic and the D. C. component of O(t) are transmitted around the loop. Therefore, for steady state operation with sinusoidal, step, ramp, or disturbance inputs, we can approximate the input to the non-linearity with equation 2.1; and the effective portion of the output from the non-linearity can be approximated by either equation 2.2 or by equations 2.3 through 2.5.

$$2.1 \quad I(t) = M + X\sin\omega t$$

$$2.2 \quad O(t) = \frac{a_o}{2} + a_1\cos\omega t + b_1\sin\omega t$$

$$2.3 \quad O(t) = \frac{a_o}{2} + C\sin(\omega t + \phi)$$

$$2.4 \quad C = \sqrt{a_1^2 + b_1^2}$$

$$2.5 \quad \phi = \tan^{-1} \frac{a_1}{b_1}$$

It will also be assumed that $G_1(s)$ represents a compensator having a transfer function of the form expressed in equation 2.6; and that $G_2(s)$ represents a motor-load combination having a transfer function of the form expressed in equation 2.7.

$$2.6 \quad G_1(s) = k_1 \frac{\pi(s + z_i)}{\pi(s + p_i)}$$

where $z_i \neq 0$ and $p_i \neq 0$

$$2.7 \quad G_2(s) = k_2 \frac{\pi(s + z_j)}{s\pi(s + p_j)}$$

where $z_j \neq 0$ and $p_j \neq 0$

The basic Laplace transform equations for such a system are:

$$2.8 \quad \overleftarrow{\mathcal{E}} = \overleftarrow{\Theta_i} - \overleftarrow{\Theta_o}$$

$$2.9 \quad \overleftarrow{I(t)} = G_1(s)(\overleftarrow{\Theta_i} - \overleftarrow{\Theta_o})$$

$$2.10 \quad \overleftarrow{\Theta_o} = G_2(s)\overleftarrow{O(t)}$$

2.2 D. C. Levels in the Output Path

In the case of step, disturbance, ramp, or sinusoidal inputs, the D. C. component of the output from the non-linear element depends only on the linear gain of $G_2(s)$ and the applied input function, and is relatively easy to evaluate.

The equation for the Laplace transform $O(t)$ can be obtained by using only the transfer functions of the linear portion of the system as in equation 2.11. Since the steady state sinusoidal components have no effect on the D. C. components in the linear portion of the system, the principle of superposition can be used to eliminate the transforms of these components when solving for the D. C. components only. The final value theorem can then be applied to obtain equation 2.12, where $\overleftarrow{O(t)_d}$, $\overleftarrow{\Theta_{id}}$, and $\overleftarrow{I(t)_d}$ represent the Laplace transforms of the non-sinusoidal components of $O(t)$, Θ_i, and $I(t)$, respectively.

$$2.11 \quad \overleftarrow{O(t)} = \frac{\overleftarrow{\Theta_o}}{G_2(s)} = \frac{1}{G_2(s)}\left[\overleftarrow{\Theta_i} - \frac{\overleftarrow{I(t)}}{G_1(s)}\right]$$

$$2.12 \quad \frac{a_o}{2} = \overleftarrow{sO(t)_d}\Big|_{s=o} = \frac{s}{G_2(s)}\left[\overleftarrow{\Theta_{id}} - \frac{\overleftarrow{I(t)_d}}{G_1(s)}\right]\Bigg|_{s=o}$$

In order to simplify the following calculations, the limits of $G_1(s)$ and $G_2(s)$ as s approaches zero can be partially evaluated to get equations 2.13 and 2.14. These results can then be substituted into equation 2.12 to get equation 2.15.

$$2.13 \quad G_1(s)\Big|_{s\to o} = k_1 \frac{\pi(s + z_i)}{\pi(s + p_i)}\Bigg|_{s\to o}$$

$$= k_1 \frac{\pi z_i}{\pi p_i} = k_{v_1}$$

$$\left.\frac{\pi(s+z_i)}{s\pi(s+p_j)}\right|_{s\to 0} = \left.\frac{\pi(s+z_i)}{s\pi(s+p_j)}\right|_{s\to 0}$$

$$= k_2 \frac{\pi z_i}{s\pi p_j} = \frac{k_{v2}}{s}$$

2.18 $$\frac{a_o}{2} = \frac{s^2}{k_{v2}}\left[\overleftarrow{\Theta}_{id} - \frac{\overleftarrow{I(t)_d}}{k_{v1}}\right]_{s\to o}$$

For a step input, or disturbance, of magnitude A, the Laplace transform of Θ_i is given by equation 2.16. For a steady state analysis, the initial time is immaterial, and consequently the Laplace transform of $I(t)_d$ can be represented by equation 2.17 and the D. C. component of C(t) can therefore be computed by equation 2.18.

2.16 $$\overleftarrow{\Theta_i} = \overleftarrow{Au(t)} = \frac{A}{s}$$

2.17 $$\overleftarrow{I(t)_d} = \frac{M}{s}$$

2.18 $$\frac{a_o}{2} = \frac{s^2}{k_{v2}}\left[\frac{A}{s} - \frac{M}{s\,k_{v1}}\right]_{s\to o} = 0$$

A similar argument can be applied to sinusoidal inputs, since in this case, Θ_{id} is zero.

For ramp inputs of magnitude B, the Laplace transform of the input is given by equation 2.19, and the D. C. component of C(t) can be evaluated by equation 2.20.

2.19 $$\overleftarrow{\Theta_i} = \overleftarrow{Btu(t)} = \frac{B}{s^2}$$

2.20 $$\frac{a_o}{2} = \frac{s^2}{k_{v2}}\left[\frac{B}{s^2} - \frac{M}{s\,k_{v1}}\right]_{s\to o} = \frac{B}{k_{v2}}$$

For an n^{th} order system, the s term in the denominator of $G_2(s)$ would be changed to s^n. Equation 2.21 can be derived for such a system by following a line of reasoning similar to that used for the first order system. Evaluation of equation 2.21 shows that the d.c. component of $\theta(t)$ will be zero for both step and ramp inputs for any system of order higher than one.

$$2.21 \quad \frac{a_o}{2} = \frac{s^n}{K_{v2}}\left[\theta_{id} - \frac{s^r}{sK_{v1}}\right]_{s\to 0}$$

2.3 D. C. Levels in the Input Path

In the preceding discussion, there was no limitation on the nature of the non-linearity represented by G_d, since the D. C. component in the output path is independent of G_d. In general, however, the D. C. level in the input path will not only depend on the nature of the system input and the characteristics of the linear portion of the system, but will also depend on the nature of the non-linear element.

In many cases the solution for the D. C. component in the input path can be extremely complicated, and may result in transcendental equations which can best be solved by graphical means (3).

It should be noted, however, that in many cases it is unnecessary to solve explicitly for the D. C. level in the input path in order to obtain the describing function curve. This fact is particularly well illustrated in the analysis of the relay servo with a ramp input, given in section 4.2. In other cases, such as the analyses for step inputs given sections 3.2 and 3.3, the solution for the D. C. level indicates that for frequency responses analysis, the D. C. level in the input path

can be ignored in [illegible] relay is treated as a symmetrical component.

CHAPTER III

THE DISSYMMETRIC RELAY SERVO

3.1 Discussion of the Describing Function.

Appendix I contains the derivation of the generalized describing function for a dissymmetric relay with the following characteristics:

1. The pull-in voltage for a positive input is not equal to the pull-in voltage for a negative input.
2. The drop-out voltage for a positive input is not equal to the drop-out voltage for a negative input.
3. The hysteresis for a positive input is not necessarily equal to the hysteresis for a negative input.
4. The positive relay output is not equal to the negative relay output.

The input vs. output characteristics of such a relay are shown in figure I-1 of Appendix I.

Since most practical relays have positive and negative outputs of equal magnitudes, no attempt was made to analyze a relay with unequal outputs. Therefore, in the remainder of this report, it will be assumed that the relay output voltages are of equal magnitude.

3.2 The Describing Function for a Relay with no Hysteresis.

The input vs. output characteristics for a dissymmetric relay with no hysteresis can be represented by figure 3.1.

Equation 2.13 shows that for a servomechanism of the type shown in figure 2.1, the D. C. component of the relay output is zero for steady state operation after the application of a sinusoidal, step, or disturbance input. Combining this result with equation I-15 of Appendix I gives:

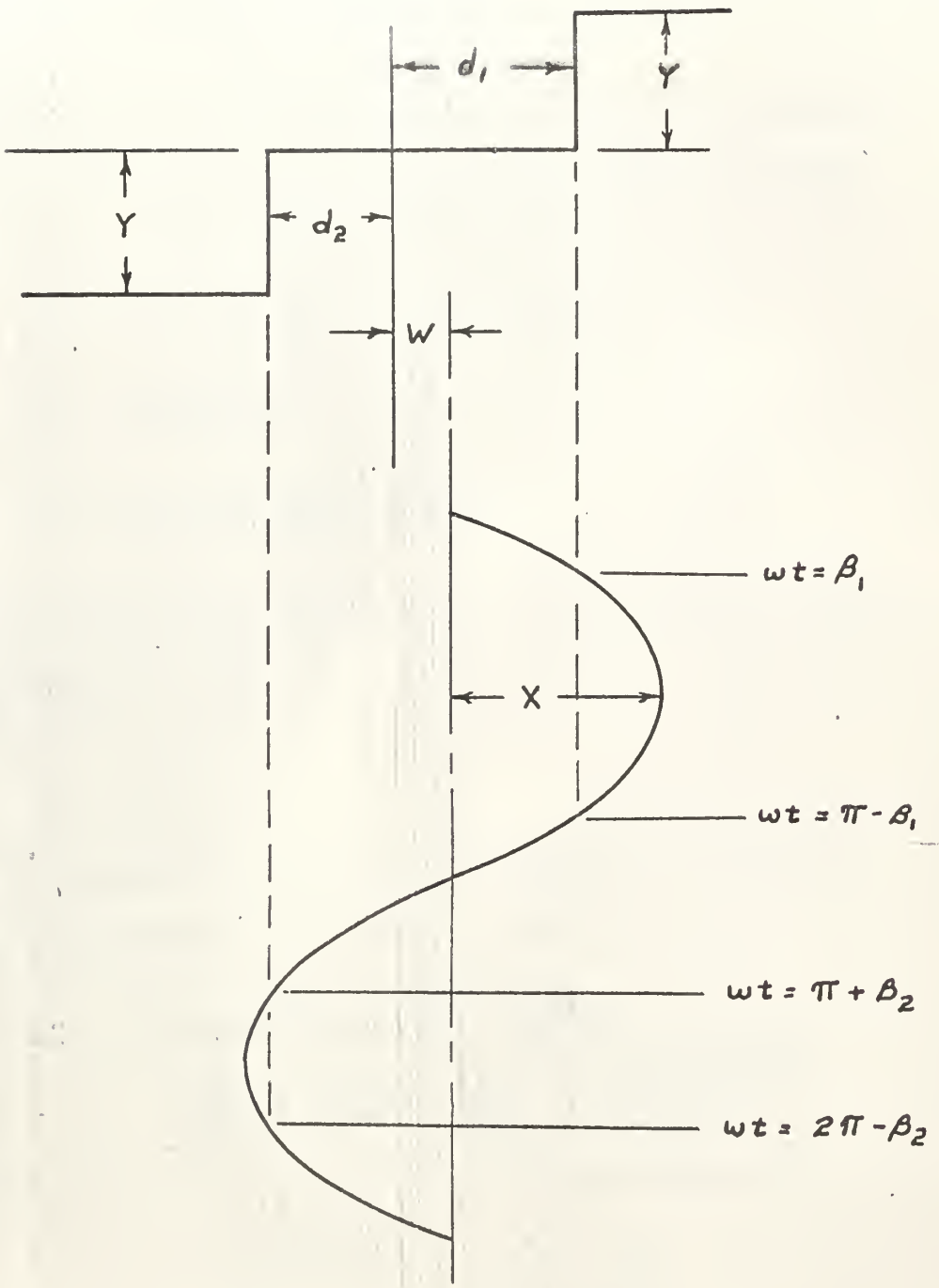

Figure 3.1 Transfer characteristics of a dissymmetric relay with no hysteresis.

3.1 $\frac{a_0}{2} = \frac{1}{\pi}(\beta_1 - \beta_2) = 0$

3.2 $\beta_1 = \beta_2$

The angle relationships of equations I-9 and I-11 of Appendix I can now be introduced to solve for the D. C. component of the input wave and to solve for β_1 and β_2 as shown below.

3.3 $\sin\beta_1 = \frac{d_1 - W}{X} = \sin\beta_2 = \frac{d_2 + W}{X}$

3.4 $W = \frac{d_1}{2} d_2$

3.5 $\sin\beta_1 = \frac{d_1 + d_2}{2X} = \sin\beta_2$

For a relay with no hysteresis the expression for a_1, as derived in Appendix I, is

3.6 $a_1 = 0$

The expression for b_1 is given by equation I-16 of Appendix I. combining this equation with equation 3.2 gives

3.7 $b_1 = \frac{2Y}{\pi}(\cos\beta_2 + \cos\beta_1) = \frac{4Y}{\pi}\cos\beta_1$

$= \frac{4Y}{\pi}\sqrt{1 - \sin^2\beta_1} = \frac{4Y}{\pi}\sqrt{1 - \left[\frac{d_1 + d_2}{2X}\right]^2}$

The equation for the generalized describing function is:

3.8 $G_d = \frac{1}{X}\sqrt{a_1^2 + b_1^2} \quad \angle \tan^{-1}\frac{a_1}{b_1}$

For the dissymmetric relay with no hysteresis, the describing function is:

$$3.9 \quad G_d = \frac{}{\pi X} \sqrt{1 - \left[\frac{d_1 + d_2}{2X}\right]^2} \quad \angle \phi$$

$$\text{for } X \geq \frac{d_1 + d_2}{2}$$

Table I is a list of the values of the generalized describing function for a relay with $d_1 + d_2 = 5.2$, and $X = 1$. A graph of this describing function is shown in figure 3.2.

X	G_d	G_d^{-1}	G_d^{-1} (db.)
2.6	0	∞	∞
3.0	.212	4.73	13.5
3.69	.257	3.89	11.5
4.0	.242	4.13	12.25
5.0	.217	4.60	13.2
6.0	.191	5.23	14.3
7.0	.169	5.92	15.4
8.0	.150	6.65	16.4
10.0	.123	8.13	17.2

Table I Values of G_d for a relay with no hysteresis.

$d_1 + d_2 = 5.2$

Equation 3.9 applies only for cases in which the relay operates on both sides during each cycle. It is not necessary to consider one-sided operation at this point, however, since this type of operation requires that the D. C. level in the relay output must be different from

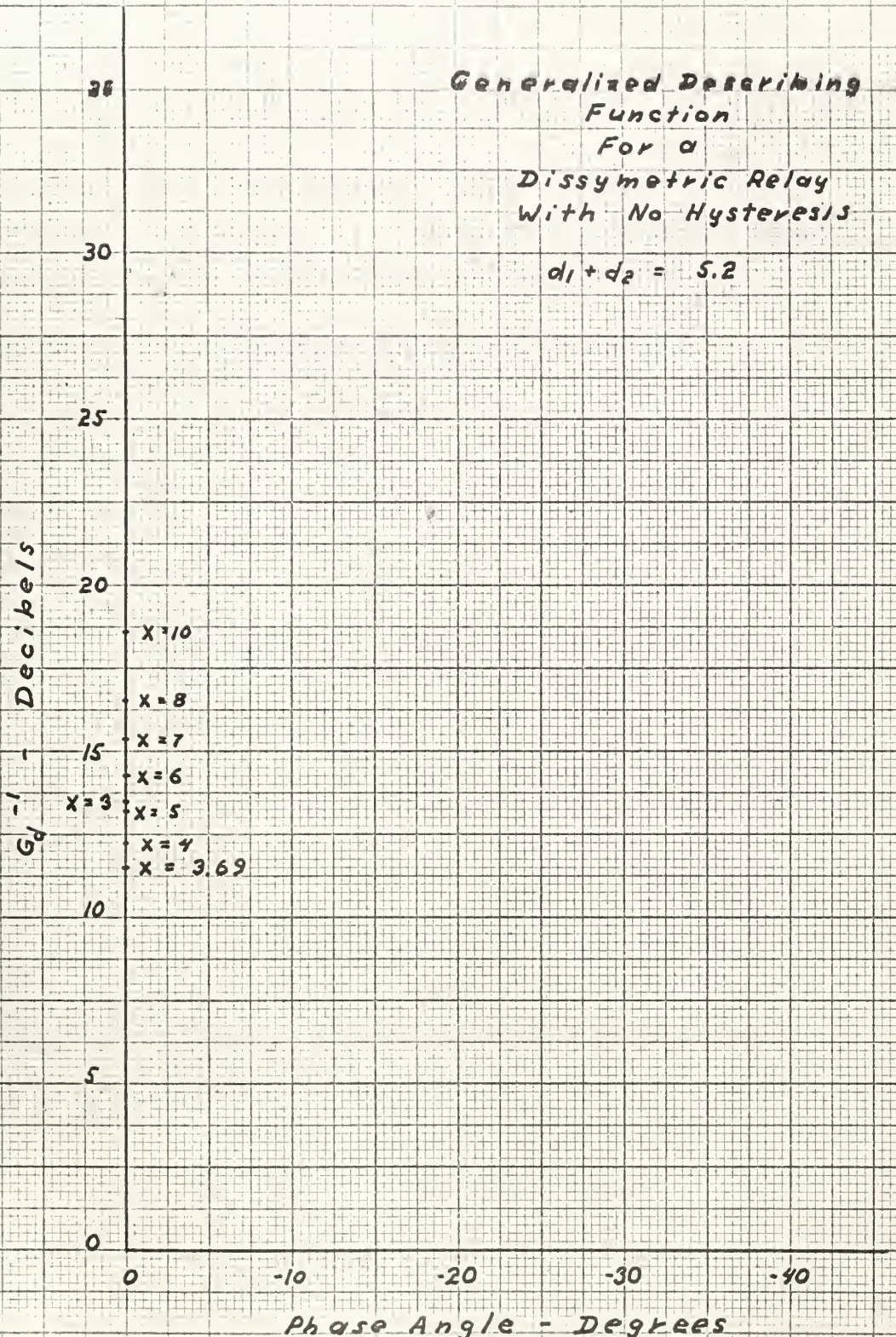
Generalized Describing Function For a Dissymetric Relay With No Hysteresis
$d_1 + d_2 = 5.2$
35
30
25
20
15
10
5
0
G_d - Decibels
X = 10
X = 8
X = 7
X = 6
X = 5
X = 4
X = 3
X = 3.69
0
-10
-20
-30
-40
Phase Angle - Degrees

Figure 3.2

zero. It has previously been shown that for a servomechanism of the type described in Chapter II, the steady state D. C. component in the relay output must be zero for sinusoidal, step, or disturbance inputs.

If the D. C. level in the output is allowed to be different from zero, as in the case of a ramp input, then both one-sided and two-sided operation is possible. The subject of ramp inputs is treated in Chapter IV.

3.3 The Describing Function for a Relay with Hysteresis.

The input vs. output characteristics for a dissymmetric relay with hysteresis can be represented by figure 3.3 . In this case, the combined results of equation 2.18 from Section 2.2, and equation I-12 from Appendix I gives:

$$3.10 \quad \frac{a_o}{2} = \frac{Y}{2\pi}(\beta_2 + \alpha_2 - \beta_1 - \alpha_1) = 0$$

$$3.11 \quad \beta_1 + \alpha_1 = \beta_2 + \alpha_2$$

Combining the angle relationships given by equations I-8 through I-11 with equation I-13 of Appendix I, we obtain equation 3.12.

$$3.12 \quad a_1 = \frac{Y}{\pi}\left[\frac{d_1 - p_1}{X} + \frac{d_2 - p_2}{X}\right]$$

If the hysteresis is the same for both sides of the relay, $d_1 - p_1 = d_2 - p_2$, and the angle relationships can be evaluated as follows:

$$3.13 \quad \sin\beta_1 - \sin\alpha_1 = \frac{d_1 - p_1}{X} = \frac{d_2 - p_2}{X}$$

$$= \sin\beta_2 - \sin\alpha_2$$

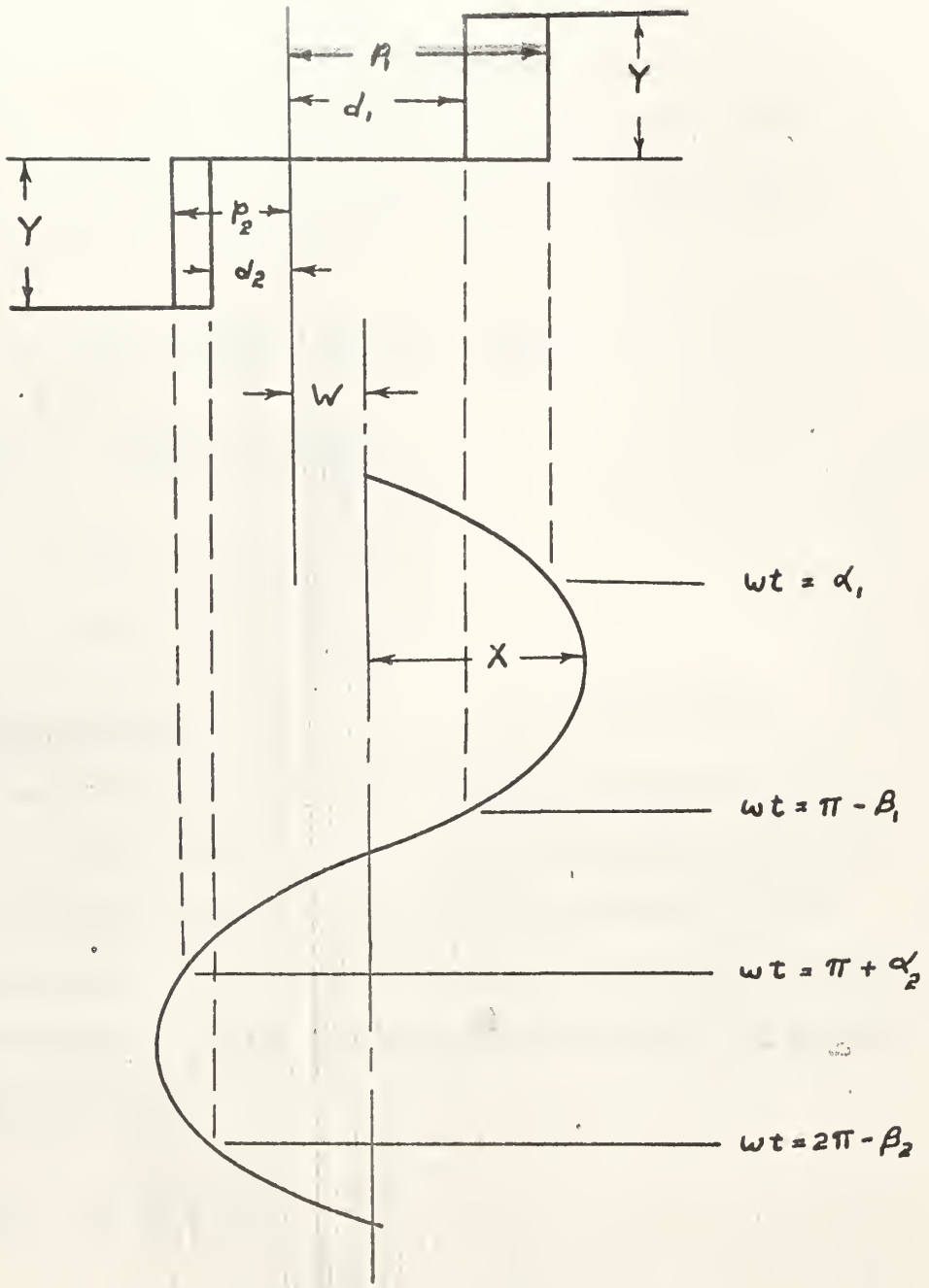

Figure 3.3 Transfer characteristics of a dissymmetric relay with hysteresis.

$$3.14 \quad \sin\beta_1 - \sin\alpha_1 = 2\sin\tfrac{1}{2}(\beta_1 - \alpha_1)\cos\tfrac{1}{2}(\beta_1 + \alpha_1)$$
$$= 2\sin\tfrac{1}{2}(\beta_2 - \alpha_2)\cos\tfrac{1}{2}(\beta_2 + \alpha_2)$$

By combining the results of equations 3.11, 3.13, and 3.14, it can be shown that $\alpha_1 = \alpha_2$ and $\beta_1 = \beta_2$. The D. C. component of the input can then be evaluated by equation 3.16, and the angles can be evaluated by equations 3.17 and 3.18.

$$3.15 \quad \sin\beta_1 = \frac{d_1 - M}{X} = \frac{d_2 + M}{X} = \sin\beta_2$$

$$3.16 \quad M = \frac{d_1 - d_2}{2} = \frac{p_1 - p_2}{2}$$

$$3.17 \quad \sin\alpha_1 = \sin\alpha_2 = \frac{p_1 + p_2}{2X} = R_p$$

$$3.18 \quad \sin\beta_1 = \sin\beta_2 = \frac{d_1 + d_2}{2X} = R_d$$

The general expression for b_1 is given by equation I-14 of Appendix I. Evaluating this equation by inserting the results from equations 3.17 and 3.18 gives equation 3.19. The describing function equation, 3.20, is then obtained by substituting equations 3.12 and 3.19 into equation 3.8. The describing function in this instance also reduces to exactly the same form as the describing function for the corresponding symmetric relay.

$$3.19 \quad b_1 = \frac{2Y}{\pi}(\cos\beta_1 + \cos\alpha_1)$$

$$= \frac{2Y}{\pi}\left(\sqrt{1 - R_d^2} + \sqrt{1 - R_p^2}\right)$$

3.20 $$N_c = \frac{2}{\pi X}\sqrt{(R_d - R_p)^2 + \left(\sqrt{1 - R_d^2} + \sqrt{1 - R_p^2}\right)^2}$$

$$\phi = \tan^{-1} \frac{R_d - R_p}{\sqrt{1 - R_d^2} + \sqrt{1 - R_p^2}}$$

$$\text{for } X \geq \frac{p_1 + p_2}{2}$$

Table II contains the values of the generalized describing function for a relay with $d_1 + d_2 = 6$ and $p_1 + p_2 = 10$. A graph of this describing function is shown in figure 3.4.

X	G_d	G_d^{-1}	G_d^{-1}(db)	Phase Angle
5	.1135	[illegible]	18.9	26.6
5.2	.1413	7.08	17.0	19.5
5.5	.1505	6.65	16.4	16.2
6	.1540	6.46	16.2	13.2
7	.148	6.75	16.7	10.1
8	.1372	7.28	17.2	8.33
9	.1265	7.9	17.9	7.15
10	.1160	8.56	18.7	6.26
11	.108	9.27	19.3	5.62
12	.100	10.0	20	5.1
15	.08018	12.22	21.7	3.97
20	.0624	16.0	24.1	2.92
30	.0422	23.7	27.4	1.92
40	.0316	31.6	29.9	1.44
50	.0254	39.35	31.8	1.15

Table II Values of G_d for a relay with hysteresis.

$d_1 + d_2 = 6$ and $P_1 + P_2 = 10$

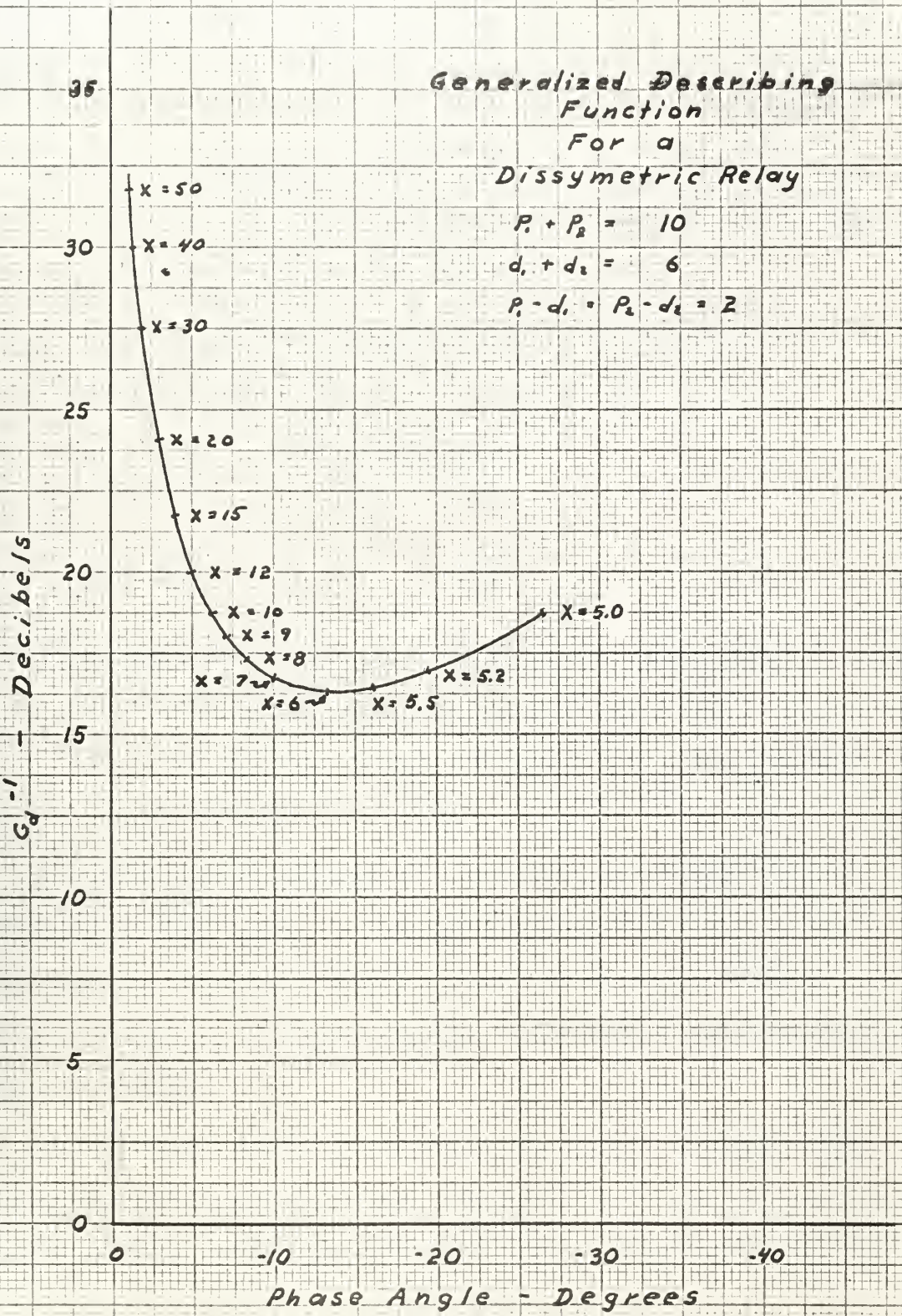
Generalized Describing Function For a Dissymetric Relay
$P_1 + P_2 = 10$
$d_1 + d_2 = 6$
$P_1 - d_1 = P_2 - d_2 = 2$
35
30
25
20
15
10
5
0
G_d -1 - Decibels
X = 50
X = 40
X = 30
X = 20
X = 15
X = 12
X = 10
X = 9
X = 8
X = 7
X = 6
X = 5.5
X = 5.2
X = 5.0
0
-10
-20
-30
-40
Phase Angle - Degrees

Figure 3.4

If the hysteresis is not the same for both sides of the relay, the transcendental equations which must be solved in order to determine the D. C. component of I(t) become much more complex. They are difficult to solve with trigonometric relationships alone, but it is relatively easy to solve them by graphical methods using the construction shown in figure 3.6. This construction can be developed in the following manner:

1. Selected a protractor with radius R.
2. Calculate the following quantities for each value of X to be investigated.

$$A = \frac{p_1 R}{X} \qquad B = \frac{d_1 R}{X}$$

$$C = \frac{p_2 R}{X} \qquad D = \frac{d_2 R}{X}$$

3. Construct figure 3.5 using the calculated dimensions.
4. Move the protractor along the vertical axis until $\beta_1 + \alpha_1 = \beta_2 + \alpha_2$ as shown on figure 3.6. This satisfies equation 3.11.

The construction guarantees that equations I-8 through I-11 are satisfied if and only α_1, β_1, α_2 and β_2 are selected as shown in figure 3.6, and the D. C. component of I(t) is established by the center of the protractor. Figure 3.6 therefore represents the desired solution for the angles, and $M = \frac{EX}{R}$.

The generalized describing function can then be evaluated using equations 3.8, 3.12, and I-14. Table III gives the values for such a describing function for a relay with $p_1 = 3$, $p_2 = 7$, $d_1 = 2$ and $d_2 = 4$. This describing function is plotted in figure 3.7.

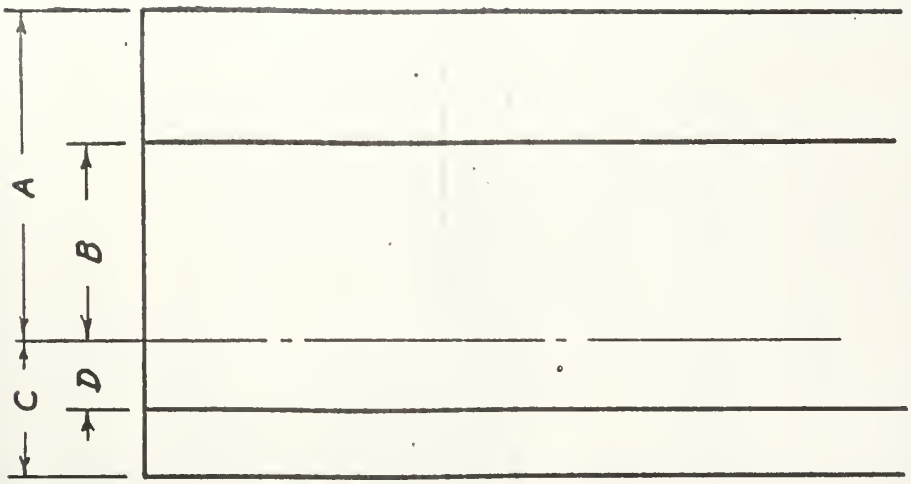

Figure 3.5

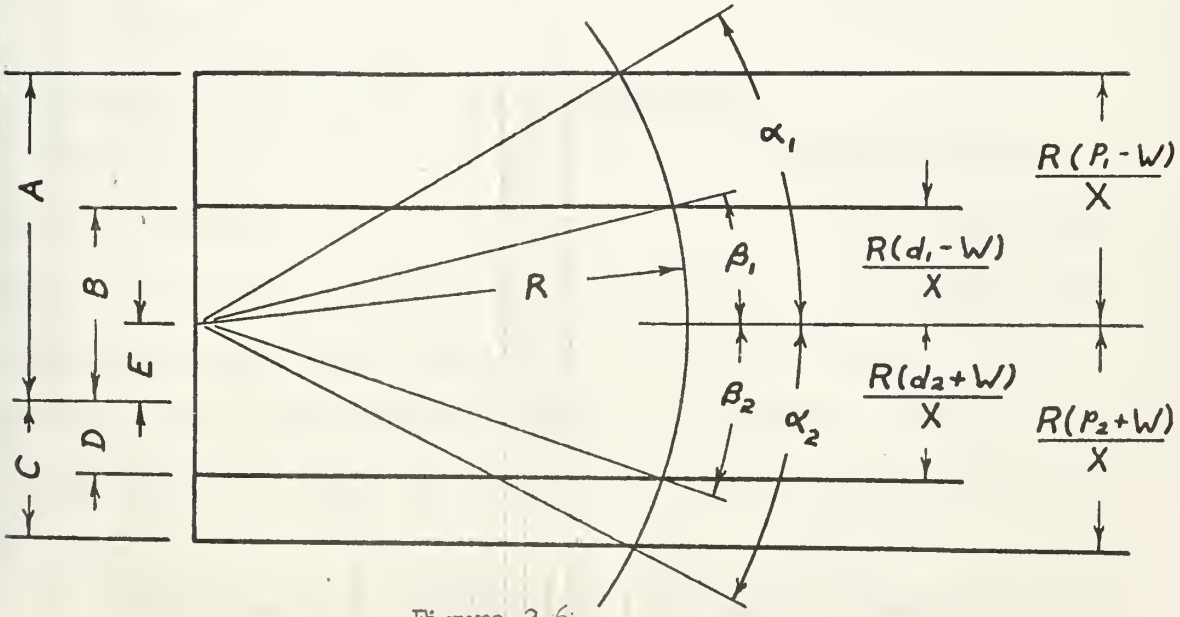

Figure 3.6

Figures 3.5 and 3.6 Graphical construction for solution of equations 3.11 and I-8 through I-11.

X	Y	G_d	$-\phi$	G_d^{-1}(db)
5.2	-1.500	.1290	21.4	17.8
6.0	-1.615	.1575	13.45	16.25
7.0	-1.562	.1525	10.2	16.25
8.0	-1.540	.1370	8.35	17.1
10.0	-1.520	.1164	6.3	18.7
12.0	-1.520	.0999	5.1	20.0
15.0	-1.510	.0813	4.0	21.7

Note: Values for G_d and ϕ for larger values of X are approximately the same as corresponding values in table II.

Table III Values of the generalized relay describing function for $p_1 = 3$, $p_2 = 7$, $d_1 = 2$, and $d_2 = 4$.

3.4 Comparison of Symmetric and Dissymmetric Relays.

Equations 3.8 and 3.20 indicate that the generalized describing functions for dissymmetric relays are exactly the same as the corresponding describing functions for symmetric relays, provided the dissymmetric relays have equal hysteresis on each side. A servomechanism containing such a dissymmetric relay would therefore respond to a sinusoidal, step, or disturbance input in a manner quite similar to a servo containing a symmetric relay.

If the servo response results in a limit cycle or sinusoidal output, the output oscillations for the symmetrical relay would be centered about the position commanded by the D. C. portion of Θ_i, while the output oscillations for the dissymmetrical relay would be offset slightly to

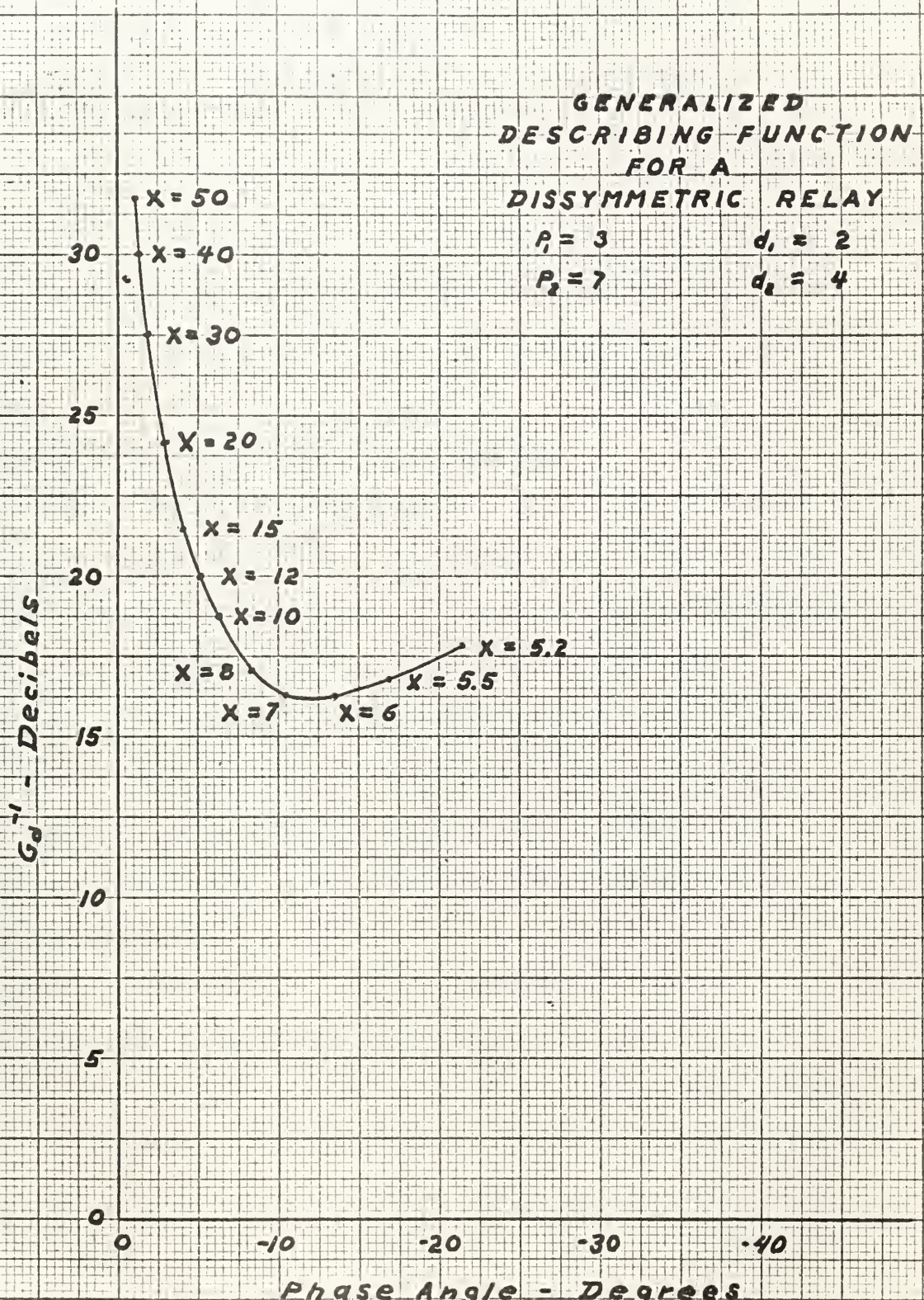
GENERALIZED
DESCRIBING FUNCTION
FOR A
DISSYMMETRIC RELAY
$P_1 = 3$ $d_1 = 2$
$P_2 = 7$ $d_2 = 4$
X = 50
X = 40
X = 30
X = 20
X = 15
X = 12
X = 10
X = 8
X = 7
X = 6
X = 5.5
X = 5.2
30
25
20
15
10
5
0
0
-10
-20
-30
-40
G_d^{-1} - Decibels
Phase Angle - Degrees

Figure 3.7

create the necessary D. C. feedback signal at the input of the relay. Thus the effect of dissymetry is to introduce a steady state D. C. error.

If the dissymetric relay does not have equal hysteresis zones on each side, the generalized describing function may be quite different from the describing function which would be obtained by assuming equal hysteresis zones and using equation 3.20. A comparison of figures 3.4 and 3.7 indicates that these differences will be relatively minor in most practical cases, and that adequate results can be obtained by using equation 3.20.

3.5 Verification of Proposed Describing Functions.

In order to verify the describing functions previously derived, a position control system consisting of the dissymmetric relay and third order linear components was postulated. Linear transfer functions with typically low pass characteristics were selected for this system.

Figure 3.8 is a schematic of the control system together with the analog computer simulation. This simulation provides for operation of the relay under varying degrees of dissymmetry and hysteresis. (4) Figure 3.9 is a Nichols Plot of the linear transfer functions with an arbitrary gain factor of 20.

Case I Dissymmetric Relay Without Hysteresis.

The relay was operated without hysteresis and with a constant total dead zone of 5.1 volts. The plus and minus pull-in voltages were varied on a series of runs to obtain various conditions of dissymmetry. Step inputs of 10 volts and 15 volts were applied to the system. The gain for the linear portion of the system was adjusted to different values so as to place the linear curve in the desired position on the

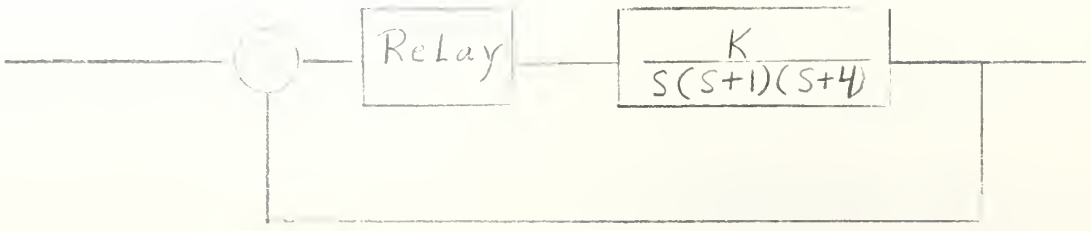

Block Diagram of Relay Servo System

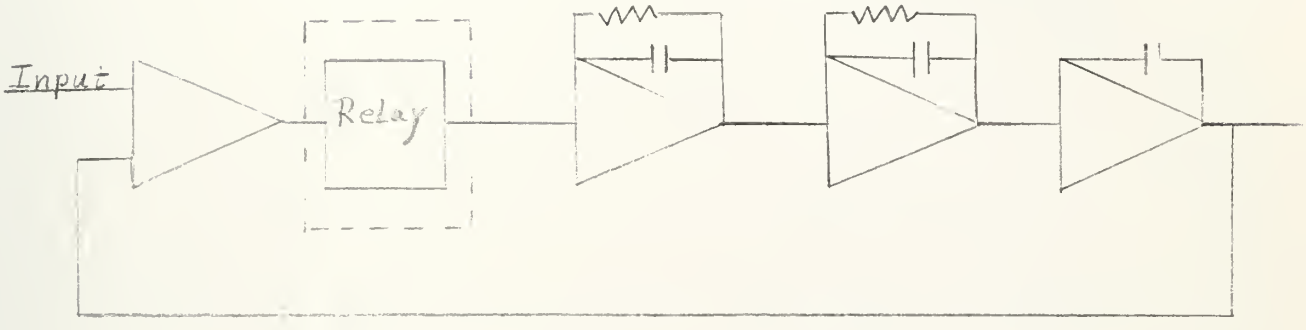

Analog Computer Schematic for Servo System Simulation

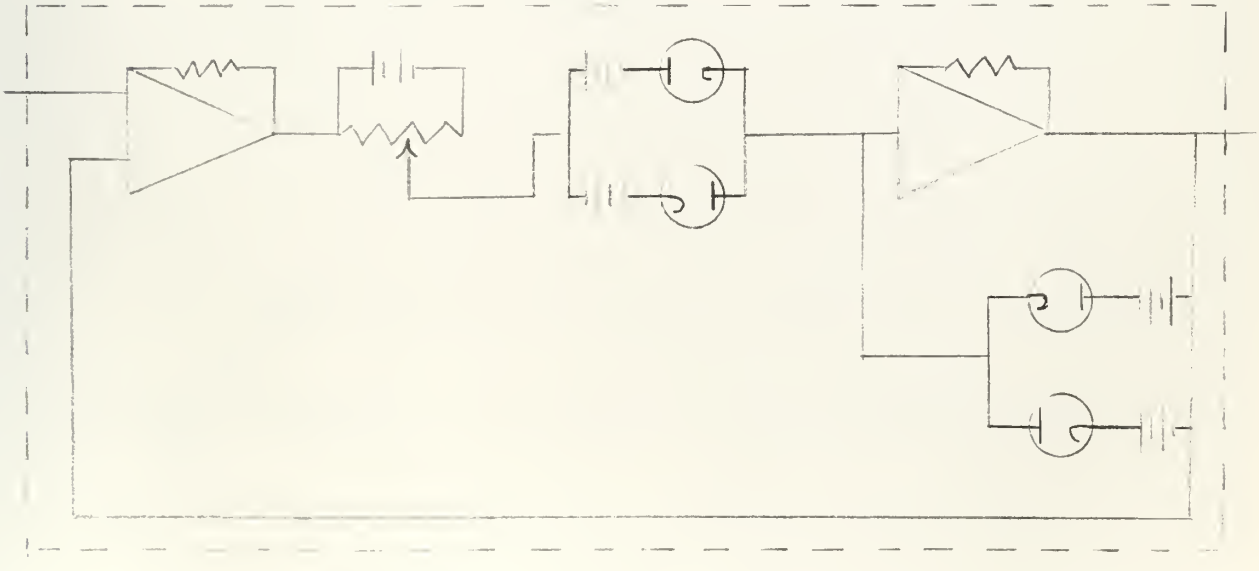

Schematic for Simulation of Relay with Variable Dead Zone and Hysteresi

Figure 3.8

Nichols Plot of linear portion of simulated relay servomechanism.

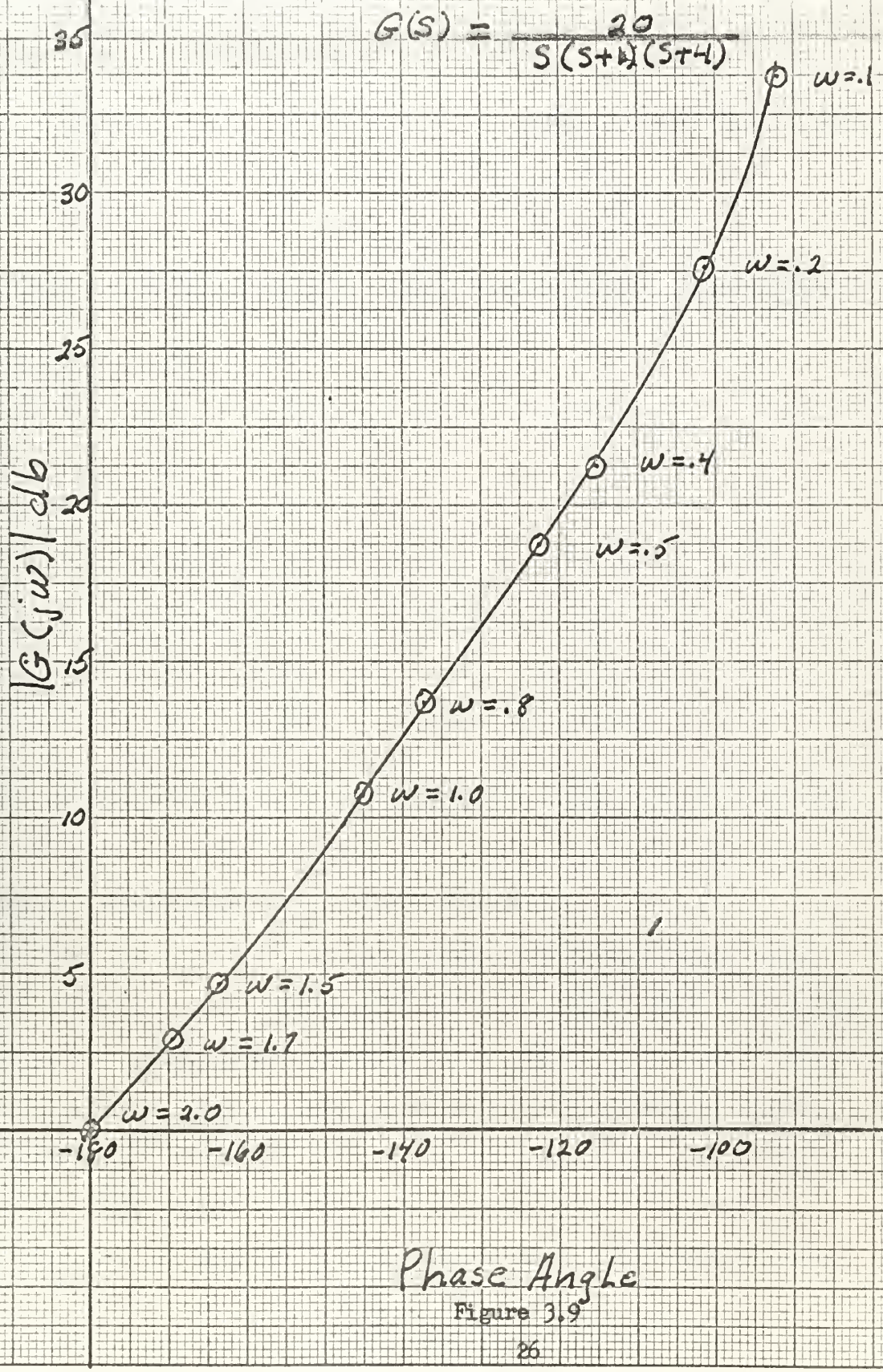

Figure 3.9

Nichols Plot, thus producing a series of limit cycles of various amplitudes.

Table IV is a summary of the results obtained. Typical Brush recordings for several values of system gain and input magnitudes are displayed in figures 3.10 through 3.12, which illustrate the predicted steady state d.c. error levels and sinusoidal characteristics.

Run	Relay Pull-in	System Gain	Observed Amplitude	Limit Cycle Frequency	Predicted Amplitude	Limit Cycle Frequency
1	+2.6,-2.5	88	4.6	2	4.7	2
2	+3.1,-2.0	88	4.6	2	4.7	2
3	+2.4,-2.7	132	8.0	2	8.0	2
4	+4.0,-1.1	132	7.9	2	8.0	2
5	+2.0,-3.1	132	8.1	2	8.0	2
6	+3.5,-1.6	132	8.0	2	8.0	2
7	+2.7,-2.4	81	4.0	2	3.8	2
8	+2.7,-2.4	63	None	-	None	-

Table IV. Experimental Results for Dissymmetric Relay Without Hysteresis.

Case II Dissymmetric Relay with Hysteresis.

The relay was operated with the following characteristics: pull in, + 3.95 volts and - 3.95 volts; drop out, + 4.0 volts and - 1.95 volts. The same general procedure was followed as in Case I. A summary of results is shown in table V. Typical Brush recordings are displayed in figures 3.13 through 3.15.

A comparison between the predicted and observed values shown in table V indicates the validity of the proposed describing function for a

relay with hysteresis. It should be noted that a small difference between the observed and predicted values is to be expected since the experimental relay characteristics were not exactly matched to those used for predictions. The predicted values were based on figures 3.4 where $p_1 + p_2 = 10$ and $d_1 + d_2 = 6$. The characteristics of the experimental relay were: $p_1 + p_2 = 9.8$ and $d_1 + d_2 = 5.95$.

Run	Gain	Observed Amplitude	Limit Cycle Frequency	Predicted Amplitude	Limit Cycle Frequency
1	620	39.6	1.88	40	1.93
2	448	29.0	1.88	30	1.90
3	300	19.85	1.75	20	1.85
4	172	12.75	1.72	12	1.75
5	37	7.15	1.50	6	1.51

Table V. Experimental Results for Dissymmetric Relay With Hysteresis.

Figure 3.10. Typical Brush recordings of step responses.

Figure 3.11. Typical Brush recordings of step responses.

Figure 3.12. Typical Brush recordings of step responses.

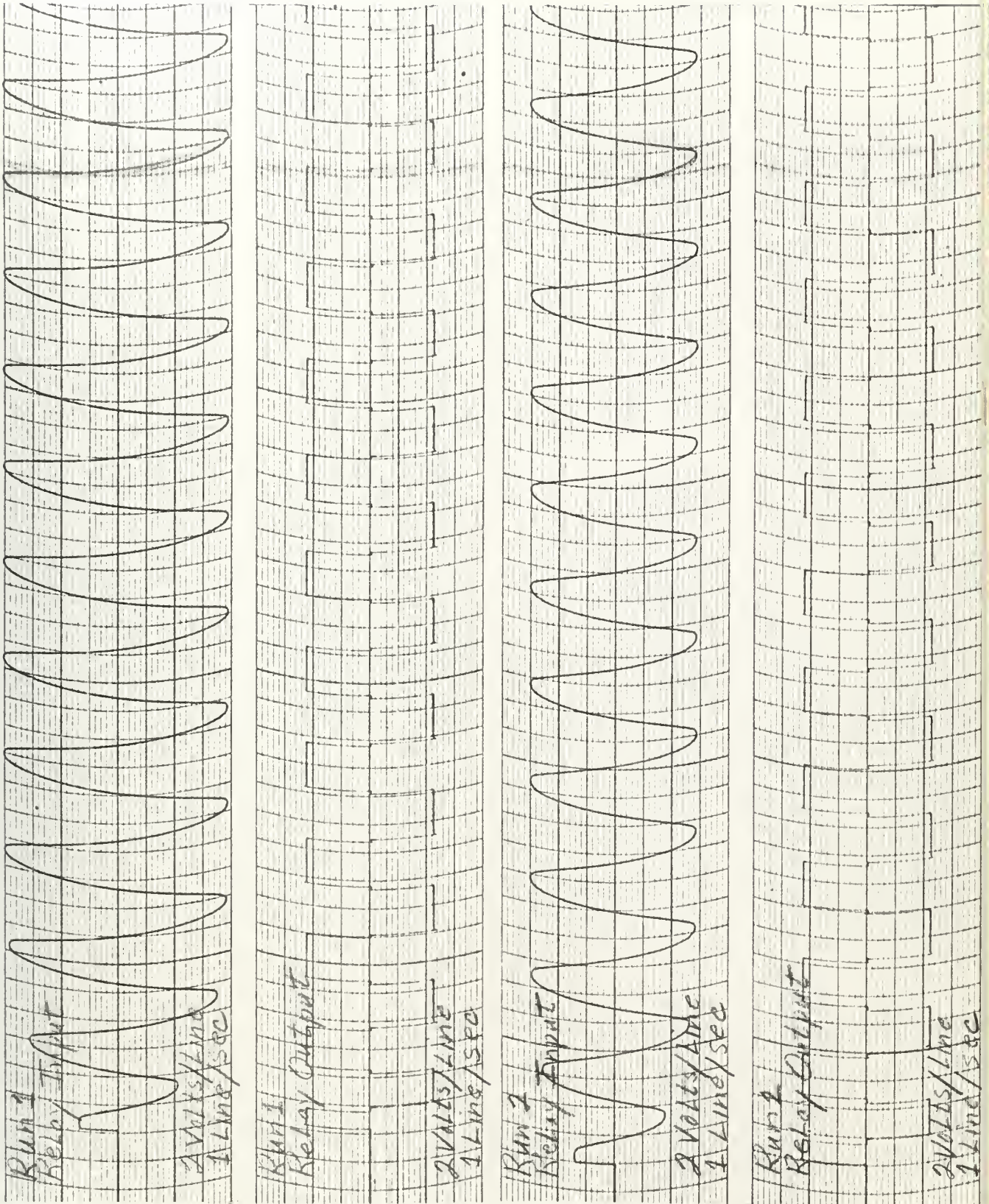

Figure 3.13. Typical Brush recordings for simulated relay servomechanism with hysteresis.

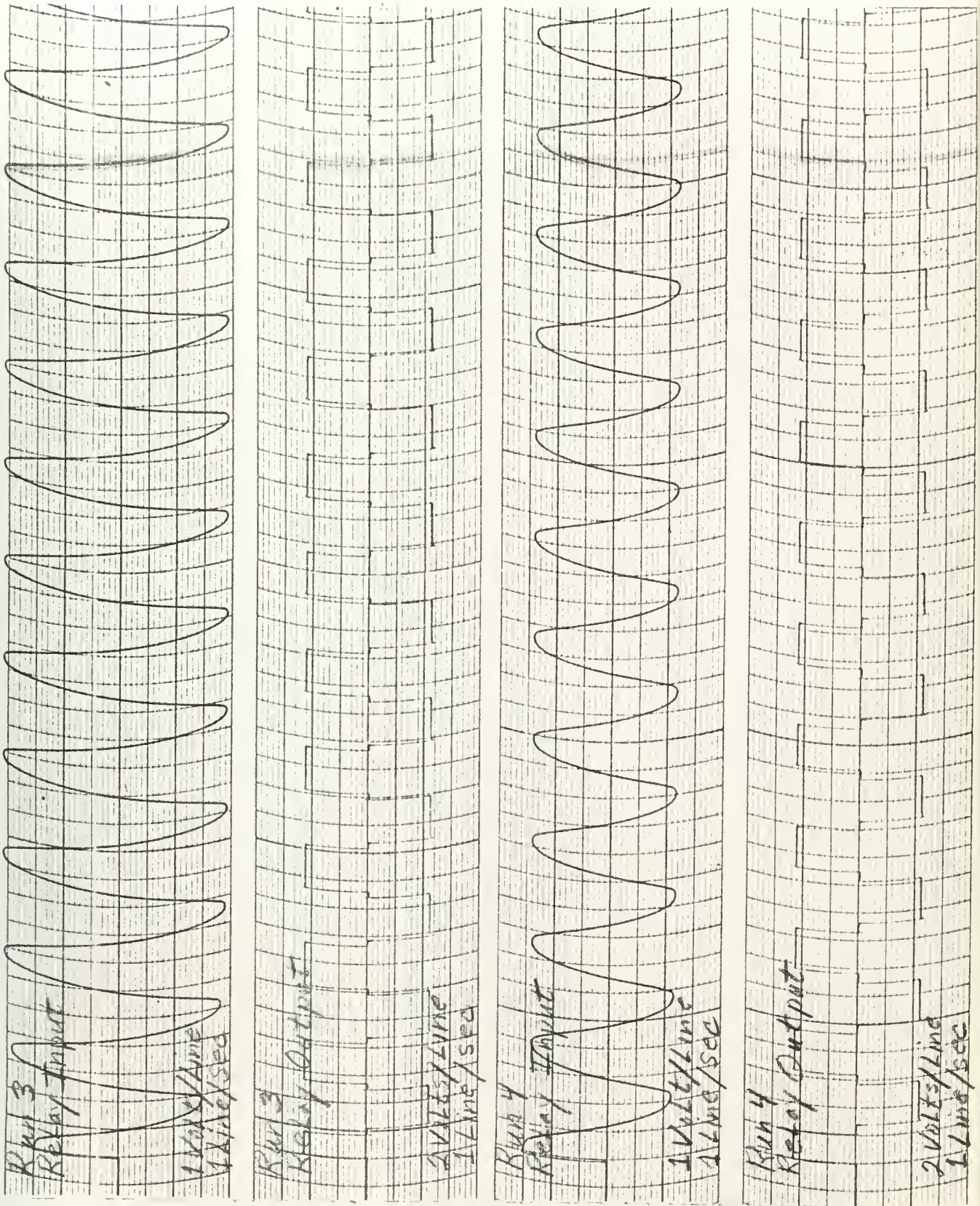

Figure 3.14. Typical Brush recordings for simulated relay servomechanism with hysteresis.

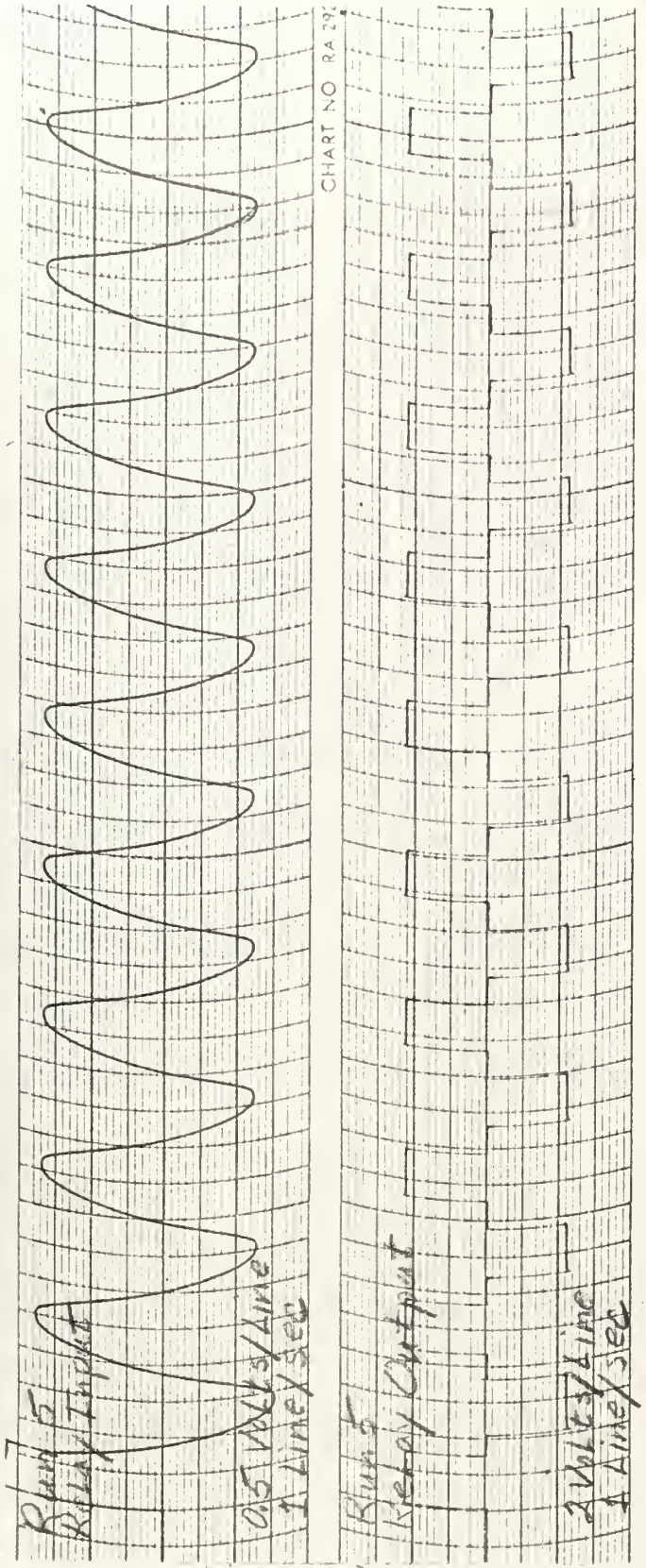

Figure 3.1. Typical Brush recordings for simulated relay servomechanism with hysteresis.

CHAPTER IV

THE GENERALIZED DESCRIBING FUNCTION FOR A RAMP INPUT

4.1 General Considerations.

When a relay servo is subjected to a step or disturbance input, the servo will either come to rest while the error remains within the limits of the dead zone, or it will enter a limit cycle which operates each side of the relay during each cycle. Similarly, when a sine input is applied, the steady state error signal will either vary within the limits of the dead zone, or it will cause the relay to operate on both sides during each cycle.

When subjected to a ramp input, however, the error will never remain in the dead zone. The servo output may come to rest, but the increasing ramp signal in the input channel will always cause the relay to actuate again. Therefore, the servo must enter a limit cycle whenever a ramp input is applied, unless the ramp signal is so large that the relay does not drop out. This limit cycle may involve actuation of both sides of the relay, or it may involve only the repeated operation of one side.

The case in which the relay operates on only one side is the simplest, and will be discussed in Section 4.2. When the relay operates on both sides, the solution must be obtained by graphical methods, as explained in Section 4.3.

4.2 Describing Function for One-sided Operation.

When the relay operates on only one side, the input vs. output characteristics can be portrayed by figure 4.1. The fourier expansion of the output wave, which is derived in Appendix I, becomes

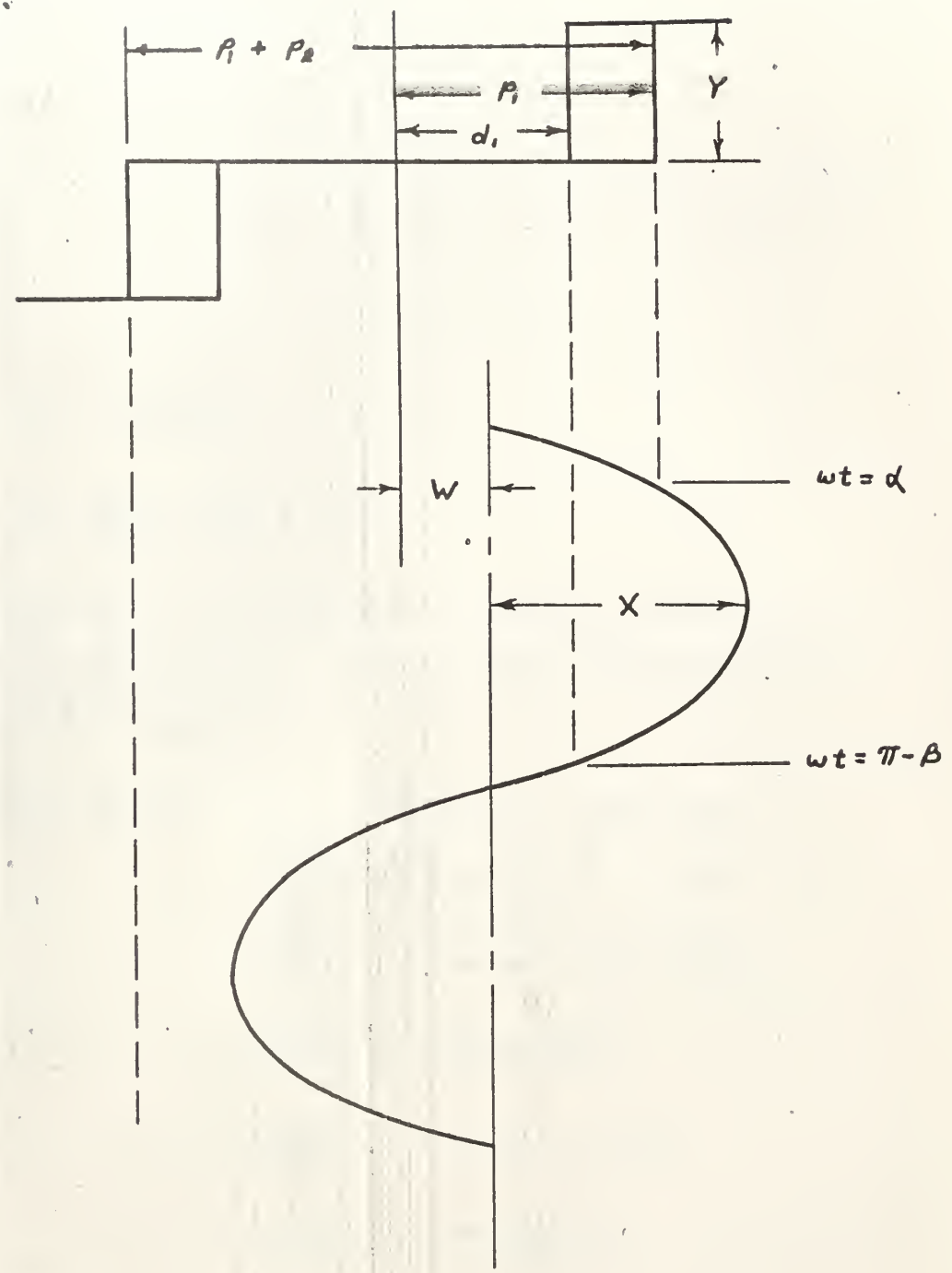

Figure 4.1 Transfer characteristics of relay operating on only one side.

4.1 $a_o = \frac{Y}{\pi}\left[\pi - (\alpha + \beta)\right]$

4.2 $a_1 = \frac{Y}{\pi}(\sin\beta - \sin\alpha)$

4.3 $b_1 = \frac{Y}{\pi}(\cos\beta + \cos\alpha)$

When the servo has a ramp input, $\Theta_i = Btu(t)$, the D. C. component of the relay output wave is given by equation 2.20. This equation can be combined with equation 4.1 to get equation 4.4

2.20 $\frac{a_o}{2} = \frac{B}{KV_2}$

4.4 $\frac{B\pi}{KV_2} = \frac{1}{2}(\pi - \alpha - \beta)$

The equations for the generalized describing function can now be obtained in the following manner, without solving explicitly for the D. C. component of the relay input.

$$4.5 \quad a_1^2 + b_1^2 = \left[\frac{Y}{\pi}\right]^2(\sin^2\beta + \sin^2\alpha - 2\sin\beta\sin\alpha) + \left[\frac{Y}{\pi}\right]^2(\cos^2\beta + \cos^2\alpha + 2\cos\beta\cos\alpha)$$

$$= \left[\frac{Y}{\pi}\right]^2(2 + 2\cos\alpha\cos\beta - 2\sin\alpha\sin\beta)$$

$$= 2\left[\frac{Y}{\pi}\right]^2\left[1 + \cos(\alpha+\beta)\right]$$

$$= 2\left[\frac{Y}{\pi}\right]^2\left[1 - \cos(\pi - \alpha - \beta)\right]$$

$$= 2\left[\frac{Y}{\pi}\right]^2\left[1 - \cos\frac{2B\pi}{KV_2}\right]$$

4.6 $\frac{a_1}{b_1} = \frac{\sin\beta - \sin\alpha}{\cos\beta + \cos\alpha} = \tan\frac{1}{2}(\beta - \alpha)$

4.7 $\phi = \tan^{-1}\frac{a_1}{b_1} = \frac{1}{2}(\beta - \alpha)$

At this point, it is convenient to introduce the trigonometric identity given by equation 4.8.

$$4.8 \quad \sin\beta - \sin\alpha = 2\sin\frac{1}{2}(\beta-\alpha)\cos\frac{1}{2}(\beta+\alpha)$$

$$= 2\sin\phi\cos\left[\frac{\pi}{2} - \frac{B\pi}{YK_{v_2}}\right]$$

$$= 2\sin\phi\sin\frac{B\pi}{YK_{v_2}}$$

$$4.9 \quad \sin\phi = \frac{\sin\beta - \sin\alpha}{2\sin\frac{B\pi}{YK_{v_2}}}$$

$$4.10 \quad \sin\phi = \frac{d_1 - p_1}{2X\sin\frac{B\pi}{YK_{v_2}}}$$

The generalized describing function for the ramp input during one-sided operation becomes

$$4.11 \quad G_d = \frac{Y}{\pi X}\sqrt{2\left(1 - \cos\frac{2B\pi}{YK_{v_2}}\right)} \quad \angle\phi$$

The relay will operate on only one side as long as X is less than a critical value, X_c, defined by equation 4.12.

$$4.12 \quad X_c = \frac{p_1 + p_2}{1 + \sin\alpha}$$

If the relay has no hysteresis, there should be no discontinuity in the describing function as the servo shifts from one-sided operation to two-sided operation. On the other hand, if the relay has a significant amount of hysteresis, there will, in general, be a discontinuity when the shift occurs.

The expression for the magnitude of G_d contains no minimum limit for the amplitude of the sinusoidal input. The phase angle expression, however, indicates that the describing function is valid only if

$$X \geq \frac{p_1 - d_1}{2\sin\frac{B\pi}{YK_{v_2}}}$$

Note that if the denominator of this expression is equal to its maximum value, 2, this restriction merely requires that the peak to peak oscillations of the sine wave must extend from one side of the hysteresis zone to the other.

For relays with absolutely no hysteresis, the describing function predicts absolutely no phase shift due to the relay. However, if the relay contains at least an infinitesimal amount of hysteresis, as all real relays do, there will be some small value of X for which the magnitude of G_d is defined, and for which the phase shift will be 90 degrees. Consequently, the effect of hysteresis must be considered to be much more significant in the case of ramp inputs than for other types of inputs.

The describing function defined by equation 4.11 can be plotted in non-dimensionalized form by defining the following quantities

$$4.13 \qquad Z = \frac{X}{p_1 - d_1}$$

$$4.14 \qquad G_{dn} = \frac{G_d(p_1 - d_1)}{Y}$$

$$= \frac{1}{\pi Z}\sqrt{2\left(1 - \cos\frac{2B\pi}{YK_{v_2}}\right)} \qquad \angle\phi$$

$$4.15 \qquad \sin\phi = \frac{-1}{2Z\sin\frac{B\pi}{YK_{v_2}}}$$

4.15 $$G(s) = \frac{Y}{p_1 - d_1} G_1(s)G_2(s)$$

4.17 $$D_h = \frac{p_1 + p_2}{p_1 - d_1}$$

The critical equation for stability becomes

4.18 $$G_d G_1(s) G_2(s) = G_{dn} G(s) = -1$$

The plot of $\left|\frac{1}{G_{dn}}\right|_{db} \angle$ can then be used as the ramp describing function for one-sided operation of any relay by simply adjusting the gain of the linear plot by the factor $\frac{Y}{p_1 - d_1}$. A graph of the describing function of equation 4.14 is plotted in figure 4.2.

The maximum value of Z for which the describing function will be valid is

4.19 $$Z_c = \frac{Y_c}{p_1 - d_1} = \frac{p_1 + p_2}{(p_1 - d_1)(1 + \sin \alpha)}$$

$$\frac{D_{hc}}{1 + \sin \alpha}$$

The describing function plot can also contain loci of equal values of $D_h = Z(1 + \sin \alpha)$. These loci will pass through points which correspond to the maximum value of Z for which one-sided operation will occur for a relay with the corresponding ratio of dead zone to hysteresis.

In order to obtain these loci, it is most convenient to first plot Z vs $Z(1 + \sin \alpha)$ for various ratios of $\frac{p}{TK_{v2}}$. This requires solving for the angle ϕ using equation 4.15 then solving for the angle α using equations 4.4 and 4.7. The values of Z can then be obtained for constant values of D_h and these points can then be plotted on the describing function

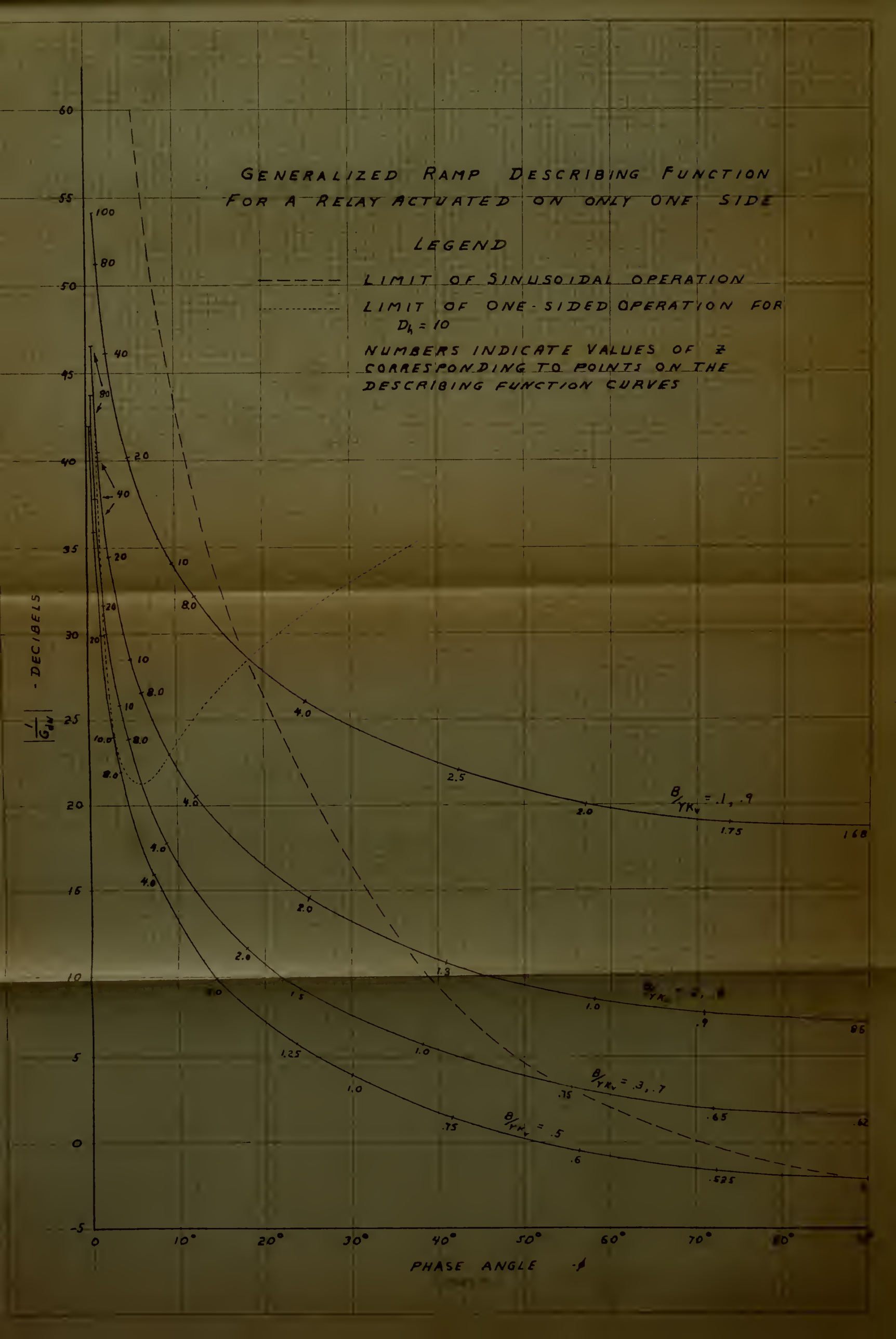
GENERALIZED RAMP DESCRIBING FUNCTION
FOR A RELAY ACTUATED ON ONLY ONE SIDE
LEGEND
LIMIT OF SINUSOIDAL OPERATION
LIMIT OF ONE-SIDED OPERATION FOR $D_h = 10$
NUMBERS INDICATE VALUES OF Z CORRESPONDING TO POINTS ON THE DESCRIBING FUNCTION CURVES
$\left|\frac{1}{G_d N}\right|$ - DECIBELS
PHASE ANGLE - ϕ
$B/YK_v = .1, .9$
$B/YK_v = .3, .7$
$B/YK_v = .5$
60
55
50
45
40
35
30
25
20
15
10
5
0
-5
0
10°
20°
30°
40°
50°
60°
70°
80°

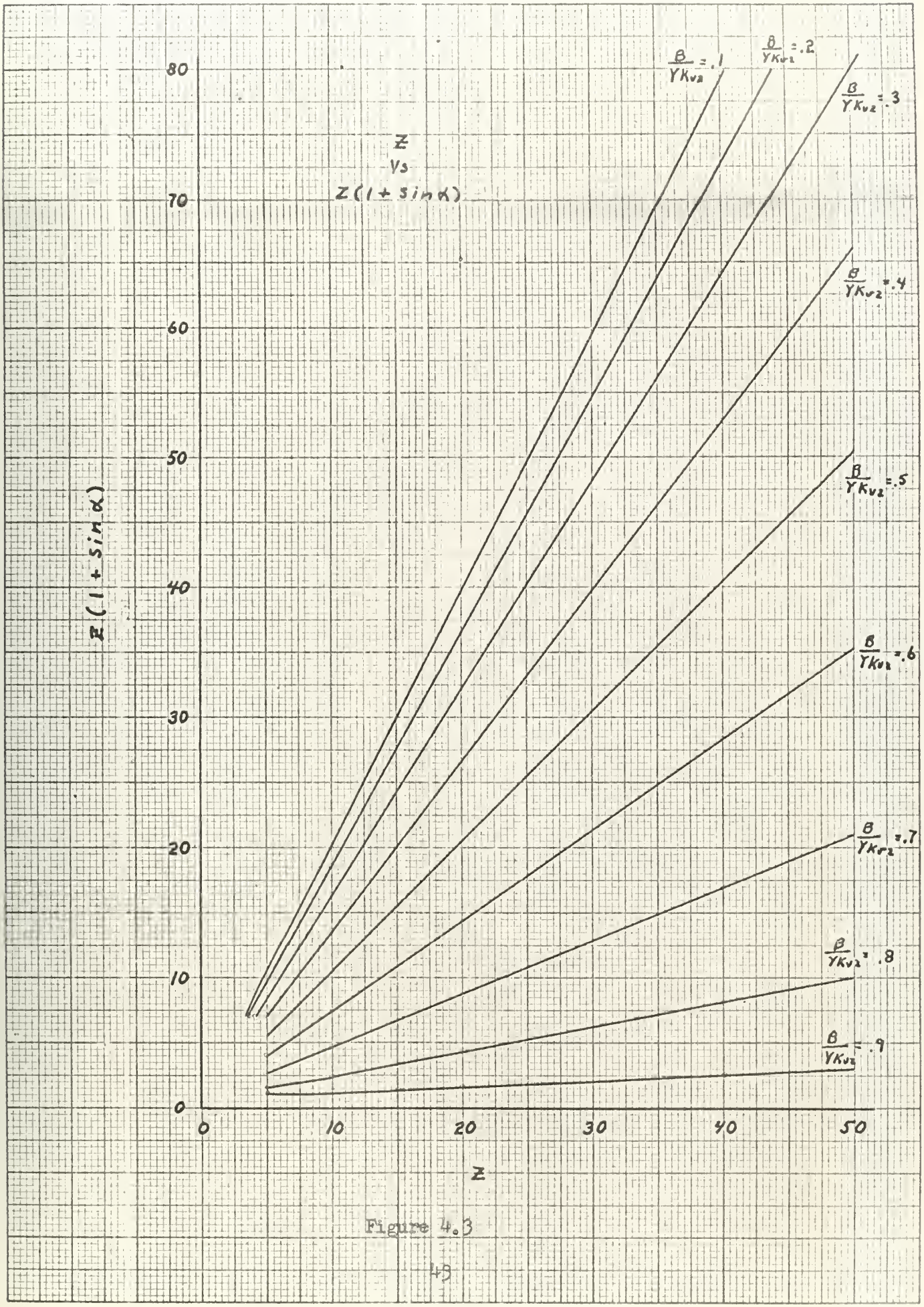
Z
Vs
Z(1 + sin α)
β/YKv2 = .1
β/YKv2 = .2
β/YKv2 = .3
β/YKv2 = .4
β/YKv2 = .5
β/YKv2 = .6
β/YKv2 = .7
β/YKv2 = .8
β/YKv2 = .9
Z(1 + sin α)
Z
0
10
20
30
40
50
60
70
80

Figure 4.3

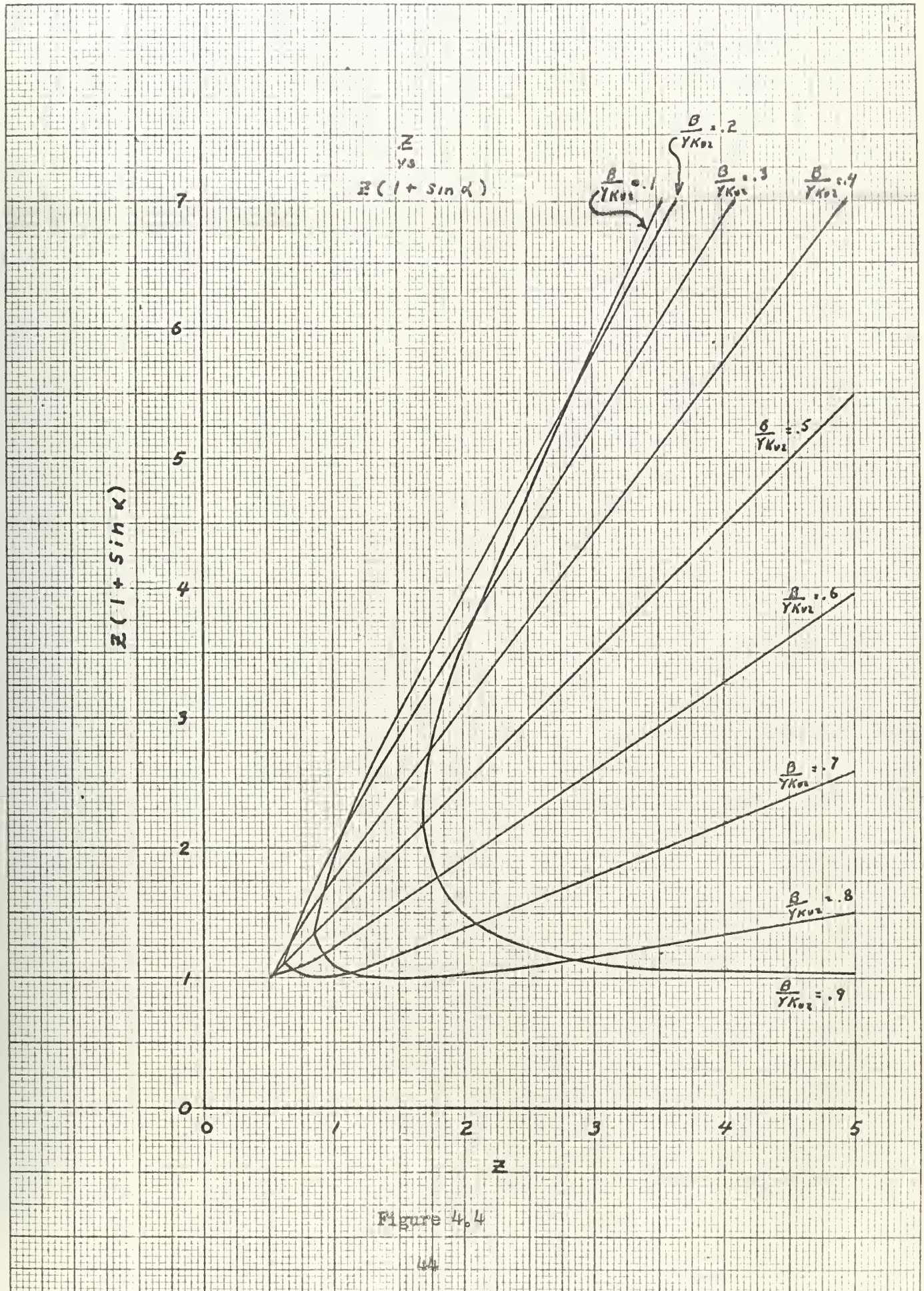
Z vs Z(1 + sin α)
Z(1 + sin α)
Z
β/YKv2 = .1
β/YKv2 = .2
β/YKv2 = .3
β/YKv2 = .4
β/YKv2 = .5
β/YKv2 = .6
β/YKv2 = .7
β/YKv2 = .8
β/YKv2 = .9
0
1
2
3
4
5
6
7

Figure 4.4

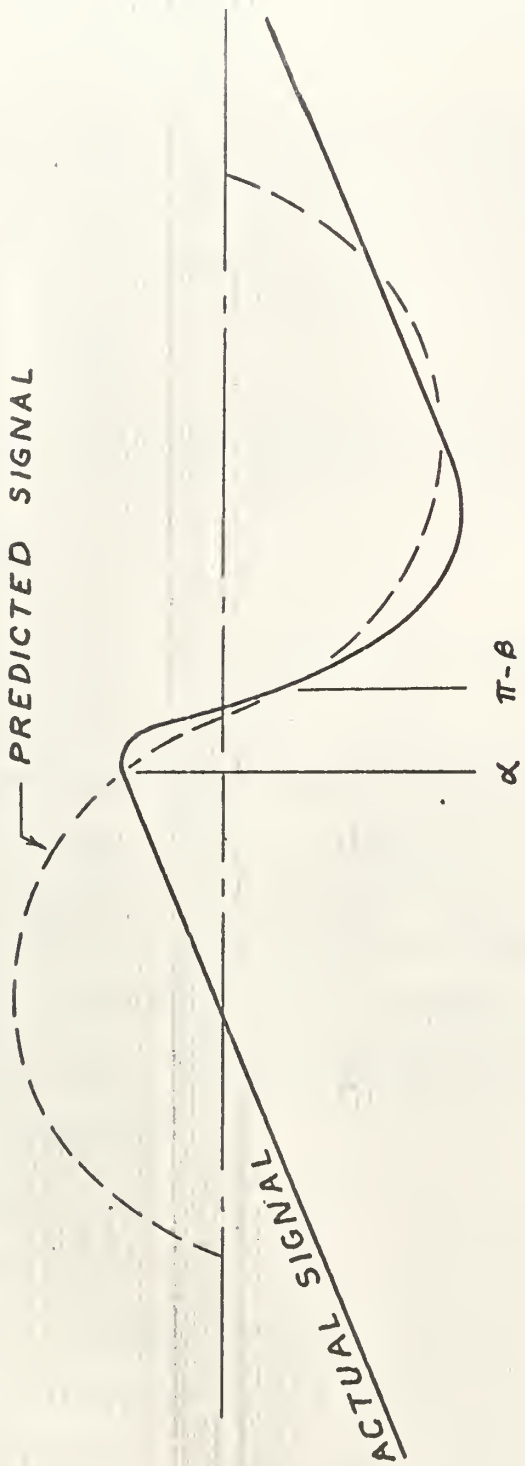

Figure 4.5 Illustration of wave shape of I(t) in non-sinusoidal region of ramp describing function plot.

curve. [illegible] are plots of Z vs $Z(1 + \sin\alpha)$ for various values of $\frac{B}{YK_{v_2}}$. The information on these curves was used to obtain the curve for $D_h = 10$, which is shown on figure 4.2.

It can also be shown that there is a limiting value of phase shift, beyond which the relay input can no longer be sinusoidal. If $B \geq .5YK_{v_2}$, sinusoidal operation is possible only if

$$4.20 \quad -\phi \leq \pi - \frac{B\pi}{YK_{v_2}}$$

If $B \leq .5YK_{v_2}$, sinusoidal operation is possible only if

$$4.21 \quad -\phi \leq \frac{B\pi}{YK_{v_2}}$$

These limiting values are also plotted on figure 4.2. The mathematical proof of the limitation is contained in Appendix II.

The non-sinusoidal characteristics become more and more pronounced as $\frac{B}{YK_{v_2}}$ approaches zero or unity, and as ϕ approaches 90 degrees. For example, for $B = .1\ YK_{v_2}$ and $\phi = 81^\circ$, the solution of equations 4.4 and 4.7 requires that $\alpha = 172^\circ$ and $\beta = 0^\circ$. This requires a wave shape of the form illustrated in figure 4.5. The corresponding sinusoidal wave is shown in dotted lines for comparison.

4.3 Experimental Procedures

As a first step toward the determination of a describing function for ramp inputs, a series of investigative runs were made on analog control systems. For this purpose two control systems were simulated with transfer functions $\frac{K}{S(S + 4)}$, and $\frac{K}{S(S + 2)(S + 4)}$, respectively. Nichols Plots for these systems are shown in figure 4.6.

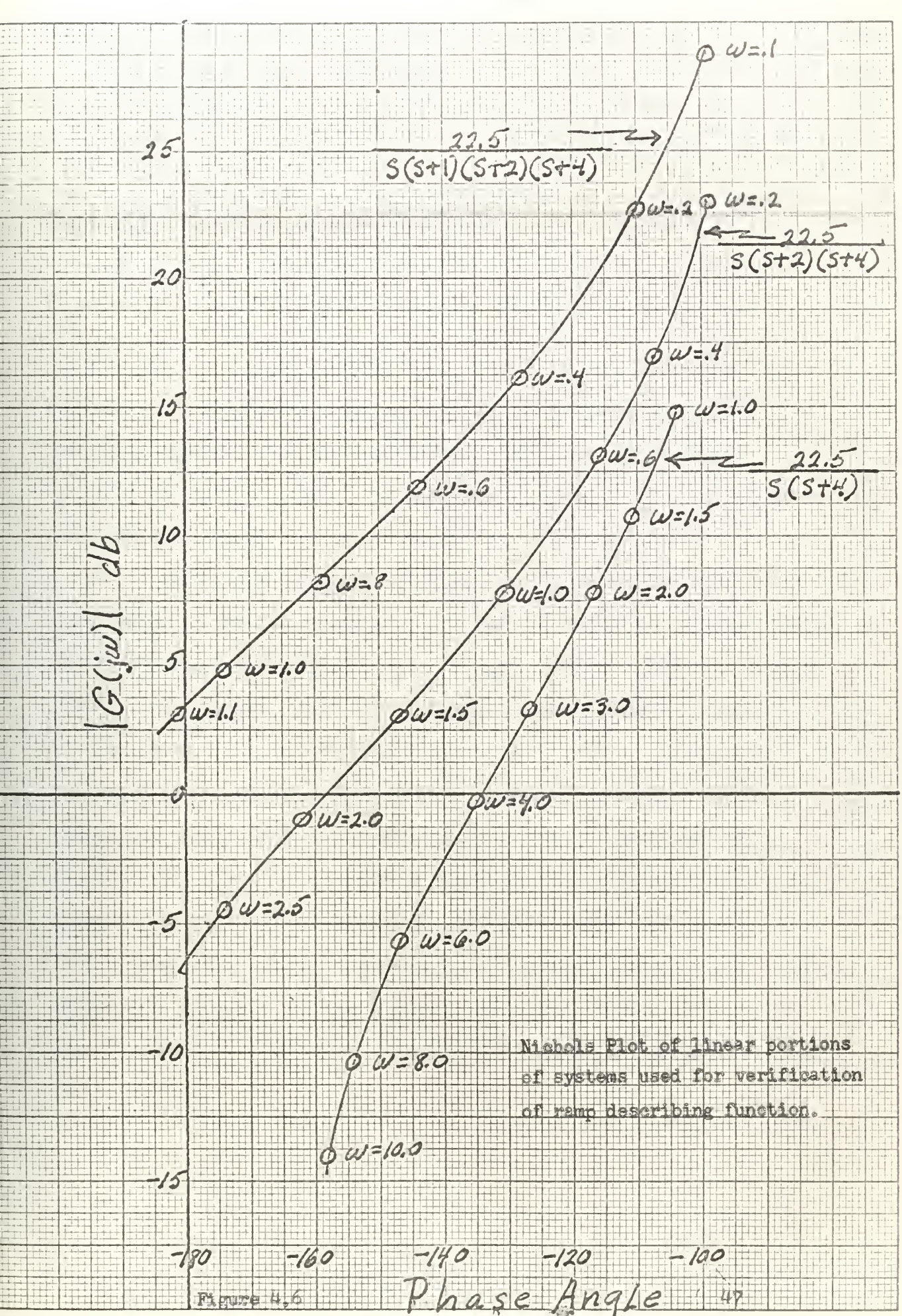

Nichols Plot of linear portions of systems used for verification of ramp describing function.

Figure 4.6

Analysis of the results of these preliminary runs together with the theoretical concepts which had been developed up to this point, indicated the significance of a parameter formed by the ratio $\frac{B}{YK_{v_2}}$. An experiment was then designed to more completely explore this feature. A series of values for the ratio $\frac{B}{YK_{v_2}}$, ranging from 0.01 to 0.90, were selected. Several runs were made at each of the selected values of the ratio, by varying B and K_{v_2} to keep the ratio constant. The relay was operated at a constant value of hysteresis and data was recorded for both the second and third order systems. The reduced data is shown in table VI, and on a Nichols Plot in figure 4.7.

An examination of the data plotted in figure 4.7 leads to the formulation of certain conclusions. Since each set of limit cycle conditions, plotted for a constant value of $\frac{B}{YK_{v_2}}$, seems to lie on a single curve it appears that a describing function curve exists for each value of this ratio. The fact that the limit cycle conditions obtained for the second order system substantiate the pattern established by the third order system even more clearly illustrates the existence of a describing function. The nature of these describing function curves indicates that they will extend across all phase angles from -90° to -180° if the curves are extrapolated beyond the region of plotted data. This agrees with intuitive reasoning that a limit cycle must exist for all type I systems with ramp inputs, unless the system is incapable of following the ramp.

		Third Order System				Second Order System			
B	$\frac{B}{VK_V}$	Freq. rad/sec	X volts	Phase Angle	Gd^{-1} db	Freq. rad/sec	X volts	Phase Angle	Gd^{-1} db
.5	.01					.924	2.0	103	34.5
.5	.02	.342	4.45	109	36.2	1.08	1.47	106	26.7
1.0	.02					1.515	1.94	111	29.9
.5	.05	.533	2.40	125	23.5	1.38	0.95	109	16.5
1.0	.05	.61	3.67	130	28.2	1.965	1.21	116	19.0
1.5	.05	.683	4.8	134	30.5	2.40	1.4	121	20.2
2.0	.05					2.73	1.56	124	21.3
2.5	.05					3.14	1.67	128	21.8
.5	.1	.64	1.65	131	15.7	1.65	.72	112	8.9
1.0	.1	.796	2.26	140	19.1	2.325	.86	120	10.9
1.5	.1	.862	2.95	142	21.7	2.86	.97	125	12.2
2.0	.1	.932	3.51	146	23.3	3.31	1.10	129	13.1
2.5	.1	.967	4.70	147	24.6	3.59	1.29	132	14.1
3.0	.1	1.03	4.60	149	30.1	3.92	1.22	134	19.1
1.5	.3	1.16	1.47	155	8.3	3.31	.62	129	1.2
3.0	.3	1.45	2.10	166	10.5	4.72	.74	140	2.3
1.5	.5	1.12	1.08	153	4.0	2.86	.57	125	-1.8
2.0	.5	1.21	1.26	156	5.6	3.40	.55	130	-1.3
2.5	.5	1.35	1.43	161	5.8	3.99	.60	135	-1.1
2.0	.7	.932	1.11	147	5.7	2.415	.57	121	- .1
2.0	.9	.472	1.16	122	11.7	.967	.62	103	6.6

Table VI. Data obtained in experimental determination of describing function for ramp input. See figure 4.7 for plot.

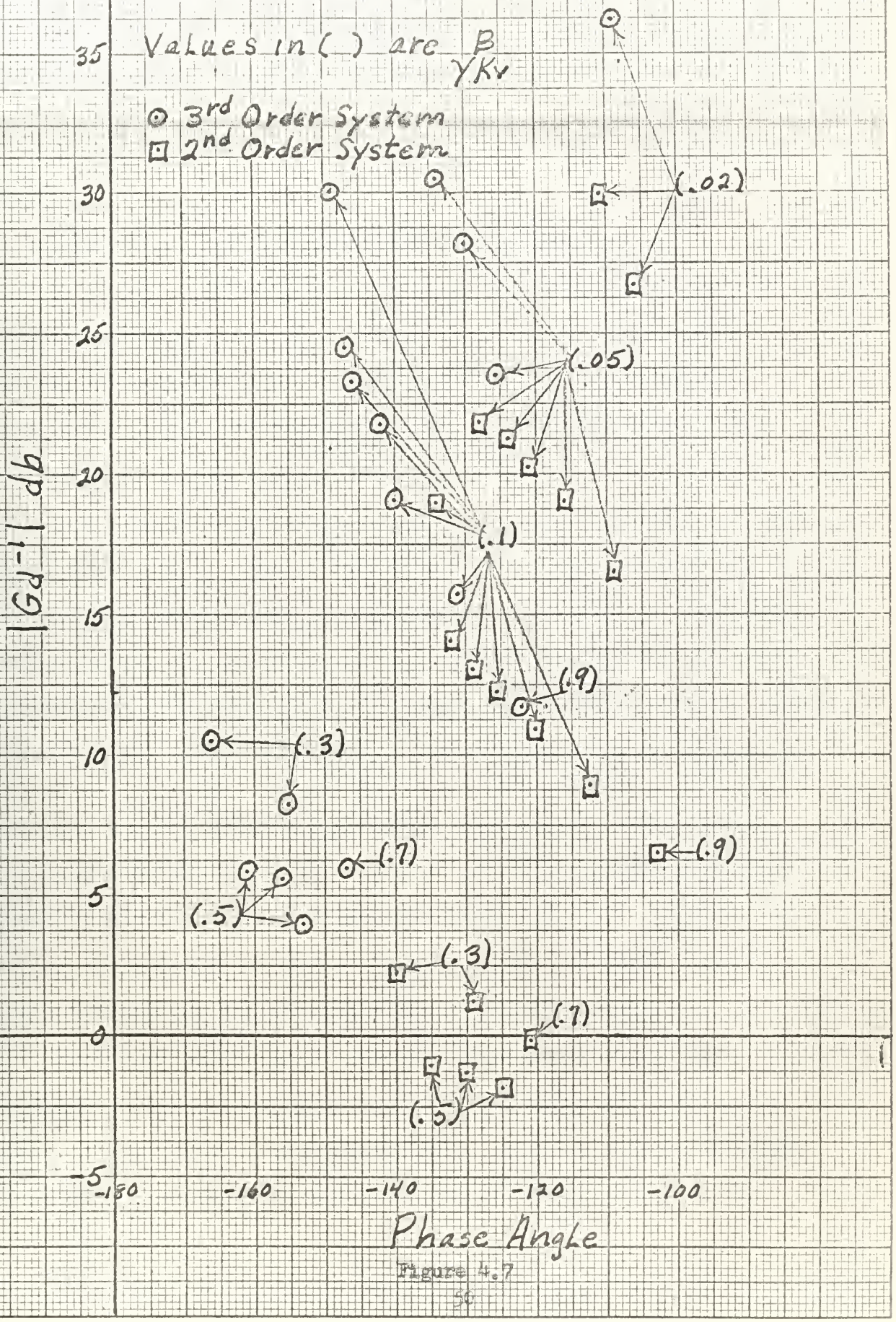
Experimental Values of Gd⁻¹
Values in ( ) are B/Kv
3rd Order System
2nd Order System
35
30
25
20
15
10
5
0
-5
|Gd⁻¹| db
-180
-160
-140
-120
-100
Phase Angle
(.02)
(.05)
(.1)
(.9)
(.3)
(.7)
(.9)
(.5)
(.3)
(.7)
(.5)

Figure 4.7

Another interesting fact observed from the plots in figure 4.7 is symmetry about the value $\frac{B}{YK_{v_2}} = 0.5$. Thus the curve for $\frac{B}{YK_{v_2}} = 0.4$ coincides with that for 0.6, the curve for 0.3 coincides with that for 0.7 etc.

4.4 Verification of the Proposed Describing Function

Although the experimental results presented in section 4.3 confirmed the existence and to some degree the nature of the describing function, another experiment was designed to explicitly verify the theoretically derived describing function. In addition to the second and third order control systems previously simulated, a fourth order system with transfer function $\frac{K}{S(S+1)(S+2)(S+4)}$ was used. In conducting these runs the gain of each linear system was held constant so that the linear curves could be superimposed on the plot of describing function curves, and the predicted limit cycles were obtained from the intersections. The value of the ramp input was varied in order to obtain different values of the ratio $\frac{B}{YK_{v_2}}$. The hysteresis was set at approximately one volt and held constant throughout. Nichols Plots of the three linear systems are shown in figure 4.6 and the nondimensionalized describing function curves are shown in figure 4.2. The predicted and observed limit cycles for each system are compared in table VII. The Brush recordings are displayed in figures 4.9 through 4.21.

Since some of the predicted limit cycle values showed discrepancies of 25% or more from those observed, it is felt that a discussion of error sources is warranted here. First of all the inherent errors of any describing function analysis are present, that is the

Run	$\frac{B}{IK_V}$	ζ	Recorded X	Recorded Freq.	Predicted X	Predicted Freq.	%Error X	%Error Freq.
			Fourth Order System					
1	.05	.281	3.16	.209	3.29	.150	3.9	23.9
2	.10	.562	3.00	.366	2.18	.44	27.3	20.2
3	.20	1.125	2.89	.61	2.12	.75	25.8	23.0
4	.30	1.687	2.79	.748	2.35	.87	15.7	8.2
5	.50	2.812	2.78	.850	2.56	.93	7.6	9.4
6	.70	3.937	2.75	.722	2.35	.87	14.5	21.0
7	.80	4.400	2.85	.572	2.12	.75	22.0	30.0
			Third Order System					
1	.05	.281	1.74	.379	3.21	.170	84.0	55.0
2	.10	.562	1.60	.679	1.77	.56	10.6	17.5
3	.20	1.125	1.49	1.17	1.32	1.22	11.4	4.3
4	.30	1.687	1.40	1.48	1.32	1.60	8.6	8.1
5	.50	2.812	1.36	1.67	1.40	1.85	2.9	10.4
6	.70	3.937	1.45	1.39	1.32	1.60	9.0	14.3
7	.80	4.400	1.53	1.07	1.32	1.22	13.7	14.0
			Second Order System					
1	.05	1.0	1.21	1.965	2.52	.75	108	62.0
2	.10	2.0	1.10	3.31	1.56	2.4	41.8	27.5
3	.30	1.5	.62	3.31	.580	3.37	6.4	1.8
4	.50	1.5	.57	2.86	.490	3.00	14.0	4.9
5	.70	2.0	.57	2.41	.504	2.40	11.5	0.4
6	.90	2.0	.62	.967	1.25	0.34	101.5	65.0

Table VII. Recorded and predicted limit cycle values for ramp inputs.

describing function predicts the ratio of the fundamental sinusoidal components of the input and output signals. In many of the runs conducted (large and small ratios of $\frac{B}{YK_V}$) the input to the non-linear element was decidely non-sinusoidal. This can be appreciated by examining the Brush recordings. It should be noted that the value recorded for the experimental value of X was simply $\frac{1}{2}$ the peak to peak amplitude of the relay input, while the value of X predicted by the describing function is the amplitude of the fundamental frequency component. Appendix II shows that for values of $\frac{B}{YK_V}$ near 0.1 or 0.9, and for values of ϕ near 90°, the pull-in angle approaches 180°, thus requiring an extremely non-sinusoidal input signal with a peak to peak amplitude which approaches $\frac{1}{2}$ the amplitude of the fundamental frequency component as illustrated by figure 4.5.

In section 4.2 and appendix II the limits for sinusoidal operation are discussed and the area defining these limits is shown on the describing function curves in figure 4.2. It can be seen from the table of predicted and observed values that the errors are largest outside the area of sinusoidal operation, and that the predicted values become increasingly more accurate as the area of sinusoidal operation is approached.

Another consideration in evaluating the discrepancies between predicted and observed values is the sensitivity of the describing function to hysteresis. The analog simulation of the relay employs two d.c. amplifiers in the analog computer, set to high gain values. It was not uncommon for the drift in these amplifiers to cause changes in the hysteresis setting of several tenths of a volt. In order to gain an

appreciation for the magnitude of errors introduced by small changes in hysteresis, a representative system containing fourth order linear components was examined. The results of this examination are shown in table VIII and graphically displayed in figure 4.8. The extreme sensitivity of the amplitude to hysteresis changes is evident. It is also noteworthy that these errors are essentially invariant with the ratio $\frac{B}{XK_{v_2}}$.

In conclusion, after careful analysis of the data recorded, it is apparent that the general validity of the proposed describing function is proven. Specifically, when intersection with a describing function curve occurs within the area defined for sinusoidal operation the amplitude and frequency of the limit cycle are predictable within 10% error. When the intersection occurs outside of this area proportionately greater errors are expected, but reasonable and useful estimates can be obtained.

4.5 The Ramp Describing Function for Two-sided Operation.

If the sinusoidal component of the relay input is greater than the critical value of X_c defined by equation 4.12 or 4.19, the system will enter a limit cycle in which both sides of the relay are actuated during each cycle. In this case, the pull-in and drop-out angles must satisfy equation 4.20, which is obtained from the simultaneous solution of equations 2.20 and I-12.

$$4.22 \quad \alpha_2 + \beta_2 - \alpha_1 - \beta_1 = \frac{2B\pi}{XK_{v_2}}$$

In order to evaluate the describing function for a relay with hysteresis it is necessary to obtain the simultaneous solution of equation 4.22 and equations I-3 through I-11. This solution can be obtained

p-d / $\frac{B}{K_v}$	.80		.90		1.1		1.2	
	%Error X	%Error W	%Error X	%Error W	%Error X	%Error W	%Error X	%Error W
.3	-30.8	-4.6	-16.3	-1.2	+15.7	+1.2	+33.6	+2.3
.4	-30.2	-2.2	-16.3	-1.1	+15.9	+1.1	+35.1	+3.3
.5	-31.3	-3.3	-16.1	-2.2	+15.7	+1.1	+35.3	+2.2
.6	-30.2	-2.2	-16.3	-1.1	+15.9	+1.1	+35.1	+3.3
.7	-30.8	-4.6	-16.3	-1.2	+15.7	+1.2	+33.6	+2.3

Table VIII. Errors in predicted amplitude and frequency resulting from small relay hysteresis errors. Zero error condition is for p-d = 1.0. Data shown is for a system with fourth order linear components:

$$\frac{2}{S(S+1)(S+2)(S+4)}$$

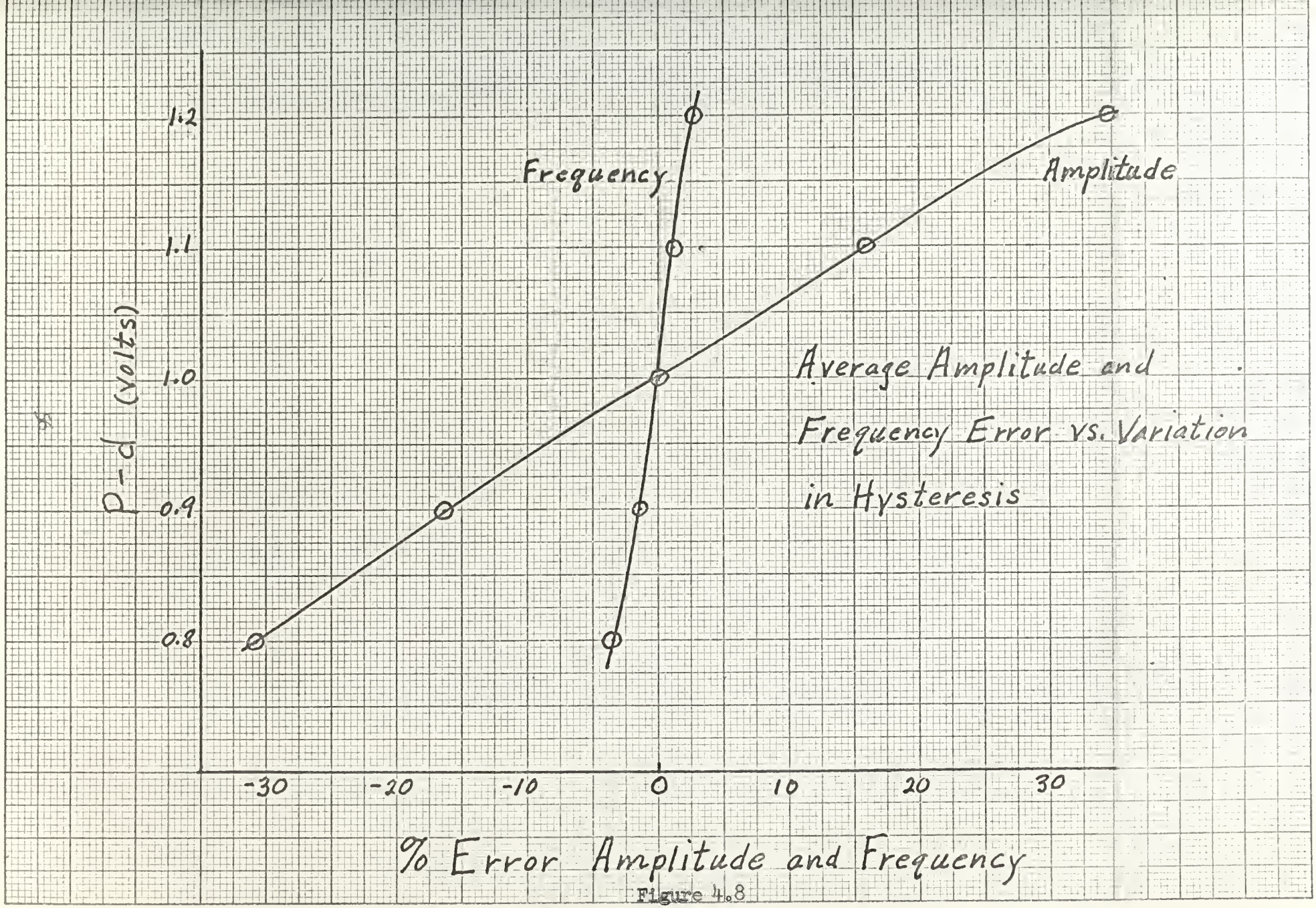
1.2
1.1
1.0
0.9
0.8
P-d (Volts)
Frequency
Amplitude
Average Amplitude and
Frequency Error vs. Variation
in Hysteresis
-30
-20
-10
0
10
20
30
% Error Amplitude and Frequency

Figure 4.8

Figure 4.7. Typical Strip Recordings of Ramp Responses.

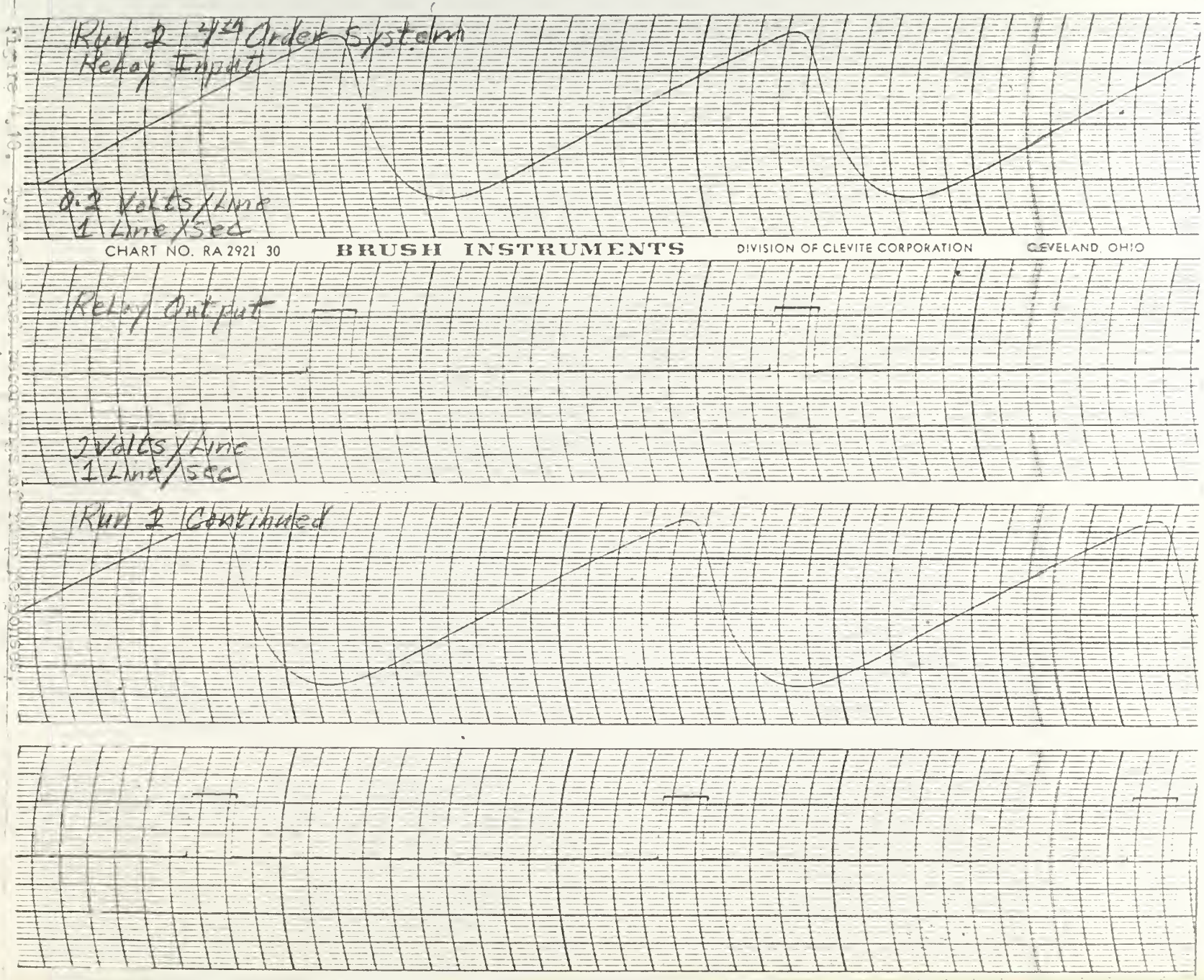
Run 2 4th Order System
Relay Input
0.2 Volts/Line
1 Line/Sec
CHART NO. RA 2921 30
BRUSH INSTRUMENTS
DIVISION OF CLEVITE CORPORATION
CLEVELAND, OHIO
Relay Output
2 Volts/Line
1 Line/Sec
Run 2 Continued

Figure 4.11. Typical Brush recordings of ramp responses.

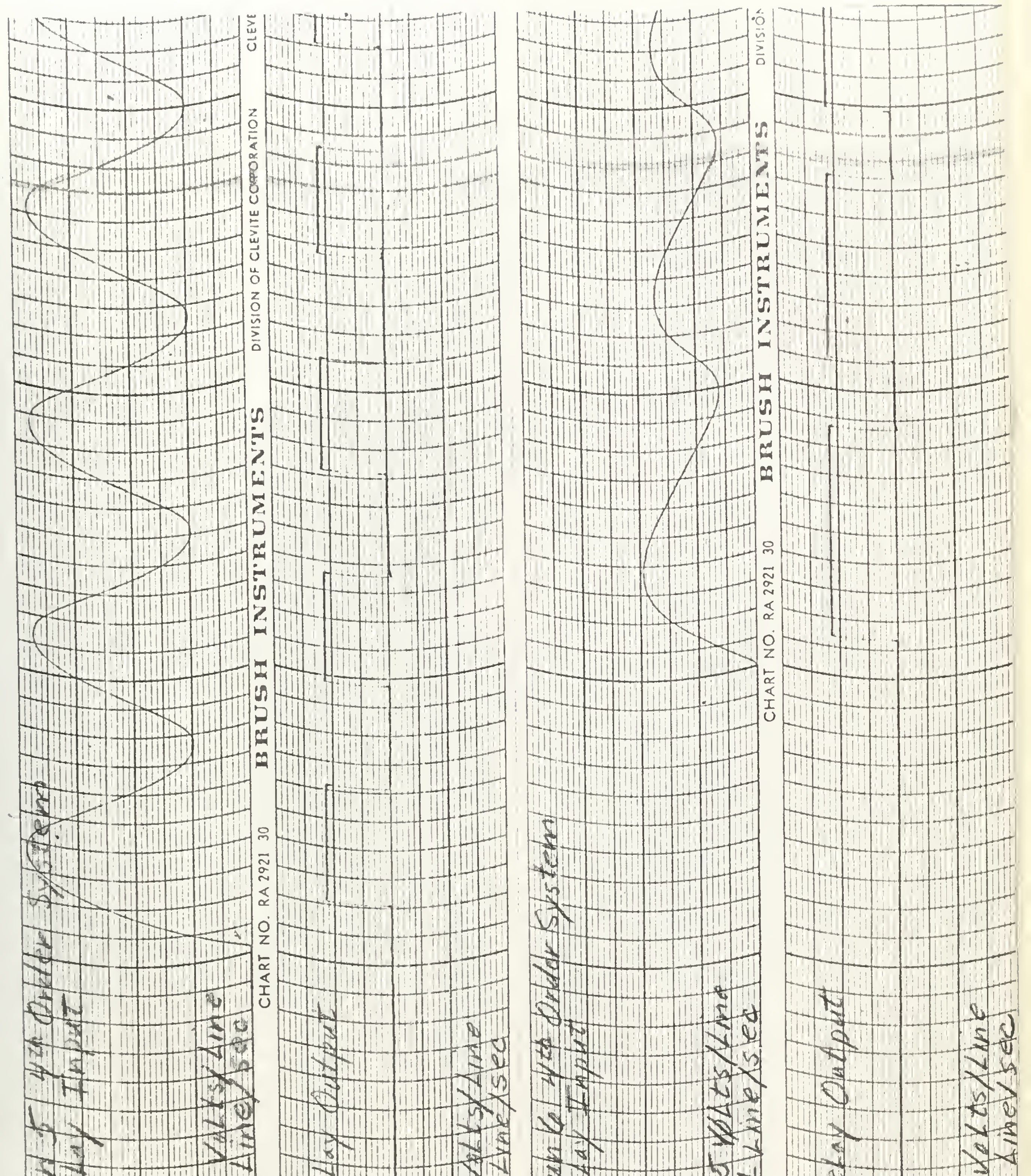

Figure 4.12, Typical Brush recordings of ramp responses.

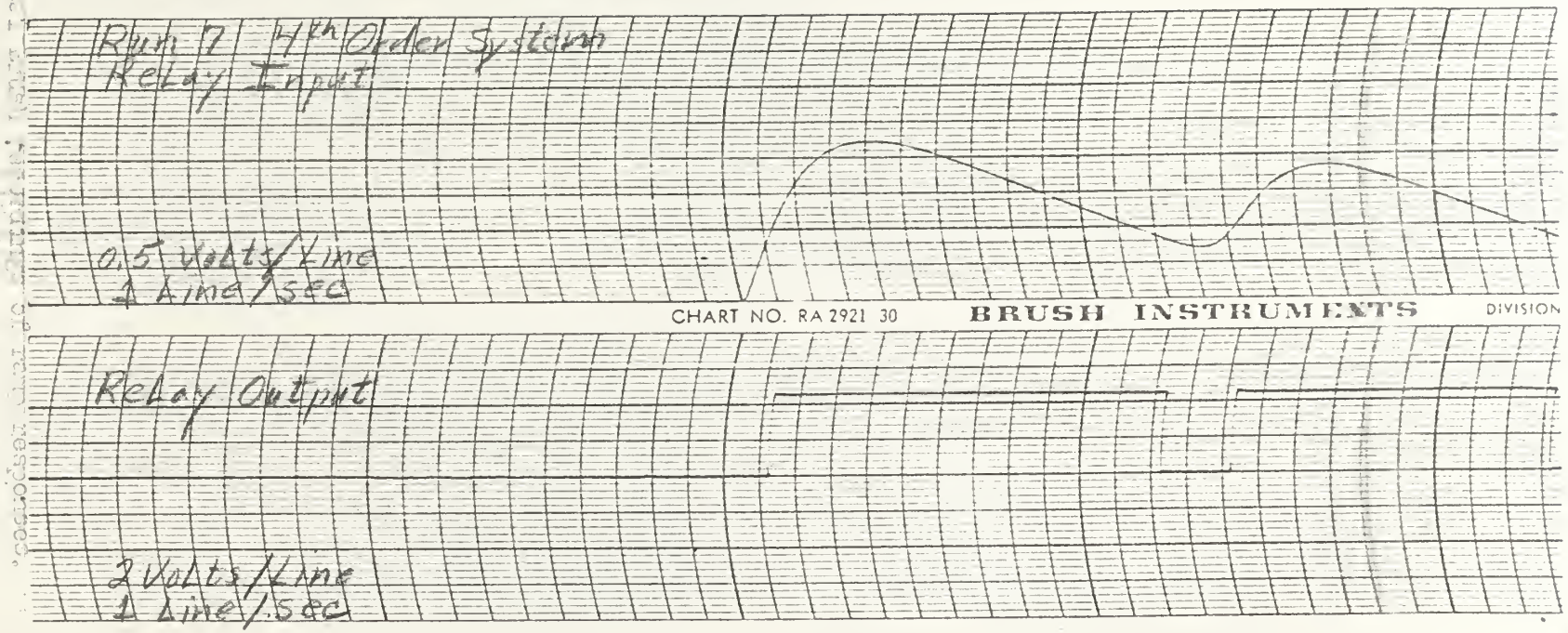
Run 7 4th Order System
Relay Input
0.5 Volts/Line
1 Line/sec
CHART NO. RA 2921 30
BRUSH INSTRUMENTS
DIVISION
Relay Output
2 Volts/Line
1 Line/.5 sec

Figure 4.14. Typical brush recordings of ramp responses.

Figure 4.15. Typical brush recordings of relay responses.

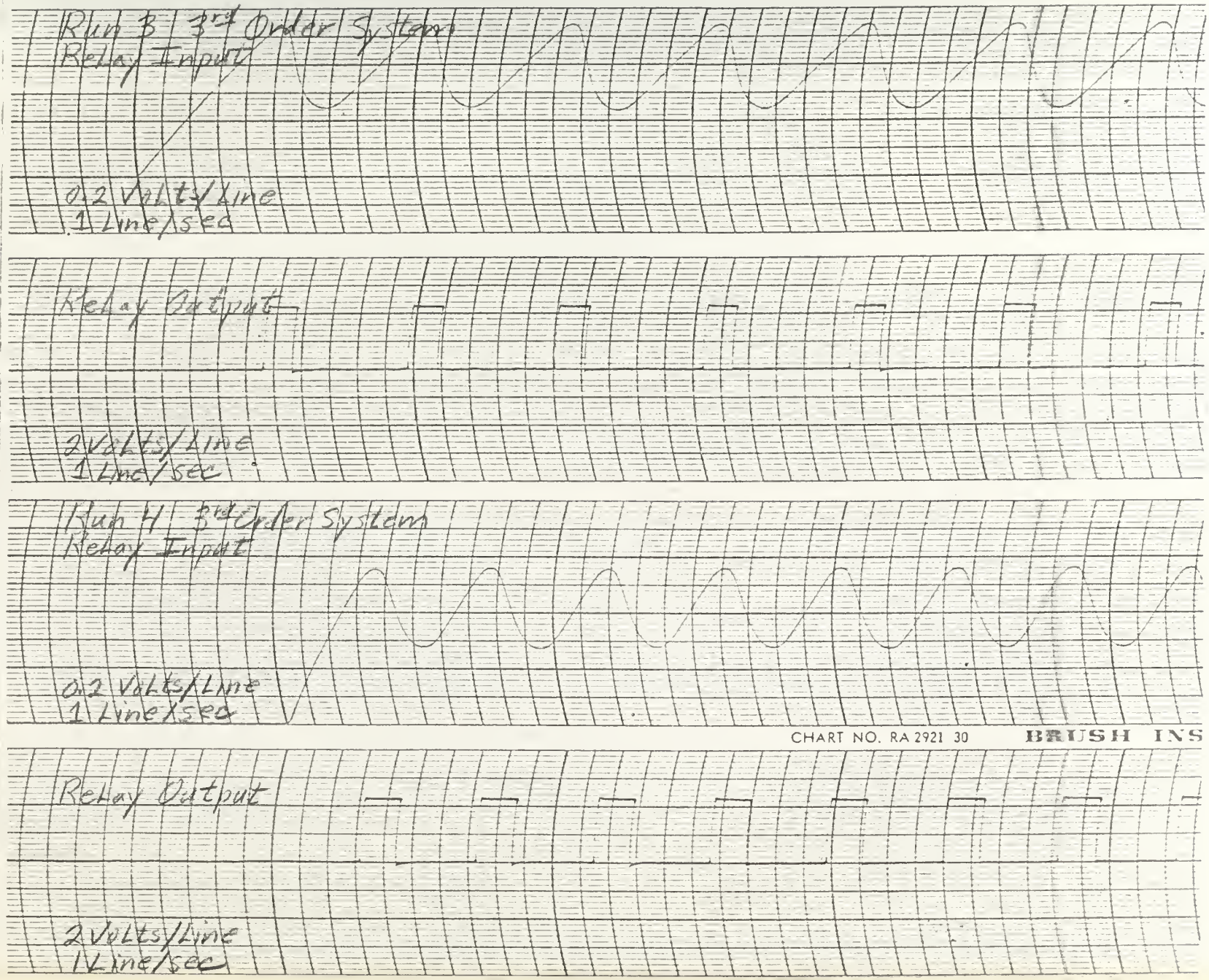

Figure 4.15. Typical Brush recordings of ramp responses.

Figure 4.17. Typical Brush recordings of ramp responses.

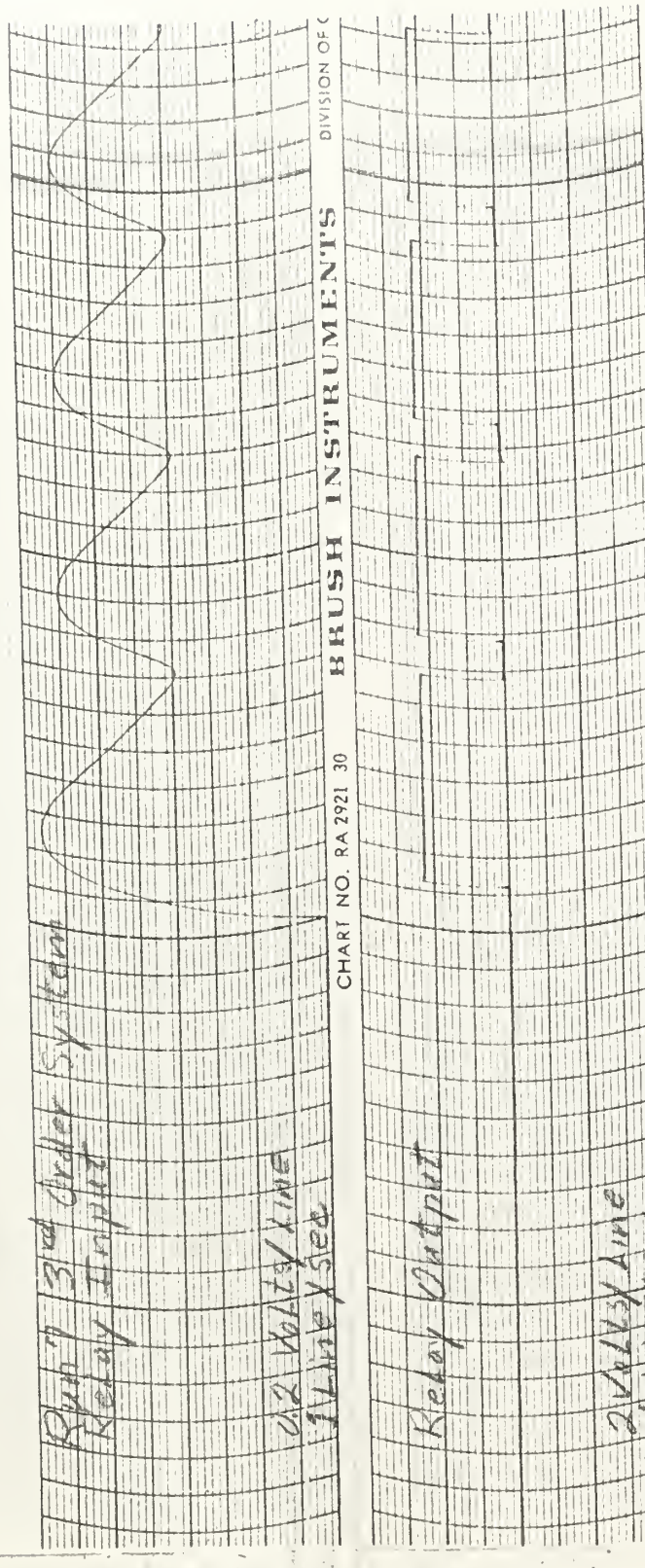

Figure 4.10. Typical Brush recordings of ramp responses.

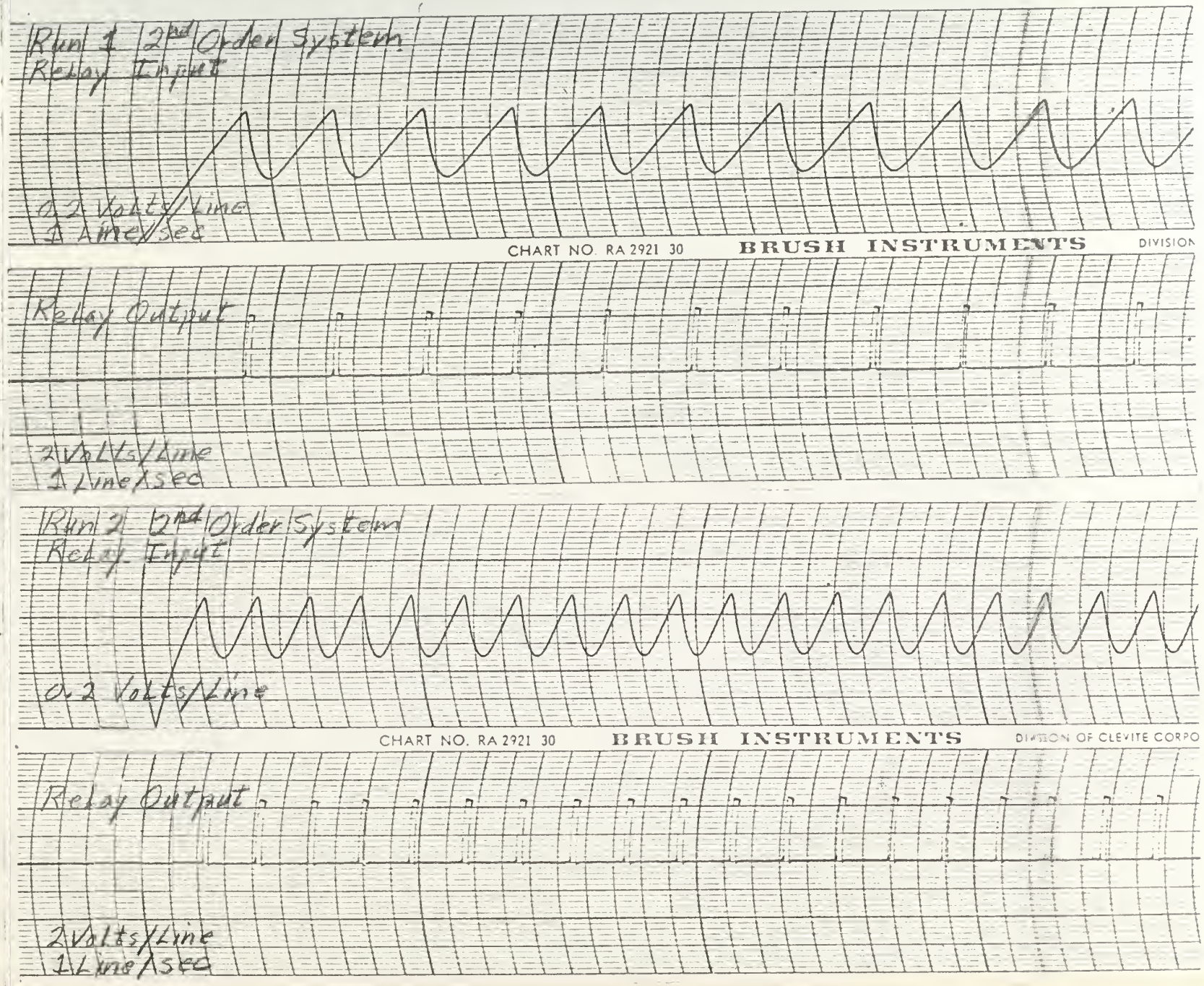

Figure 4.15. Typical Brush recording of relay responses.

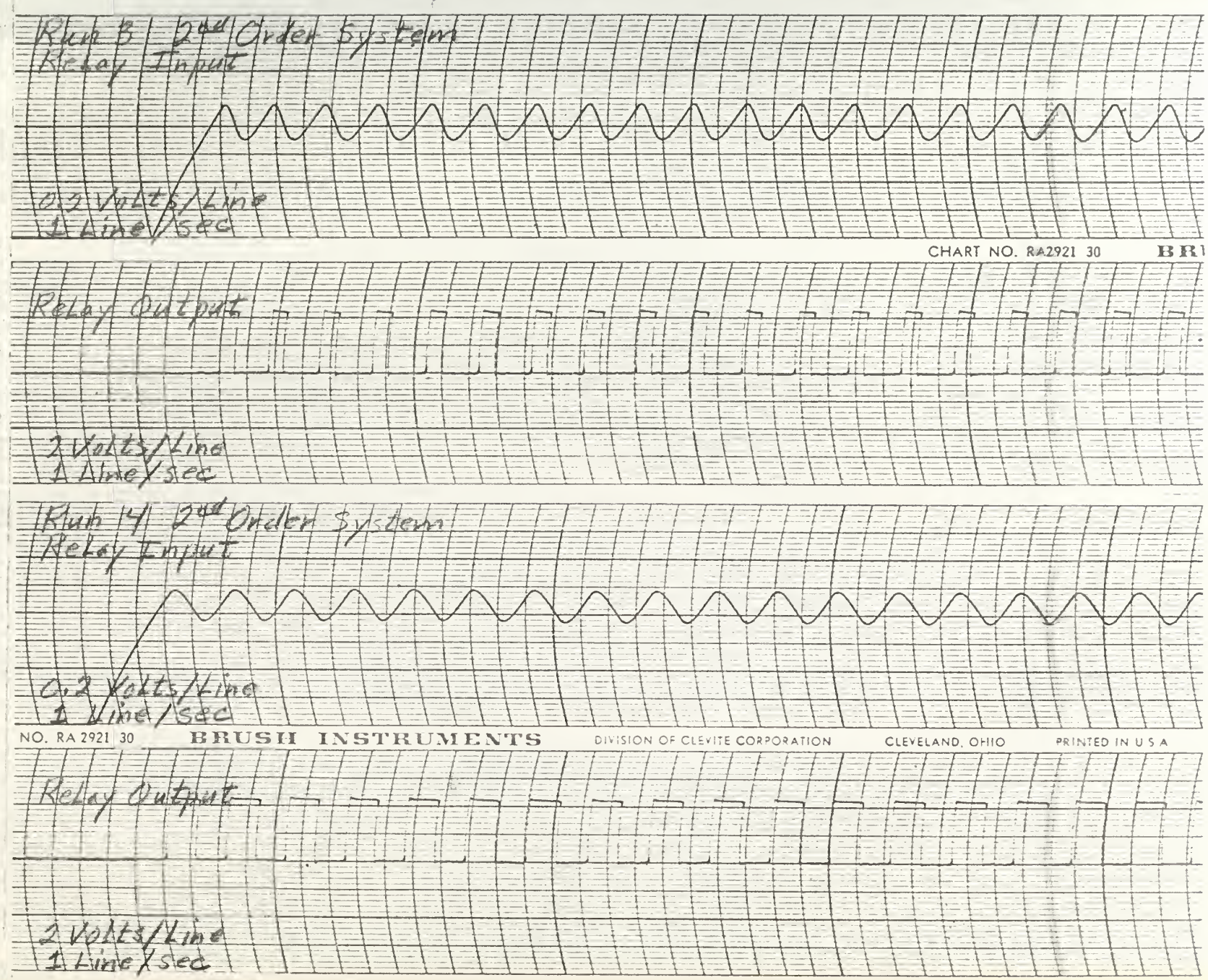
Run B | 2nd Order System
Relay Input
0.2 Volts/Line
1 Line/sec
CHART NO. RA2921 30
Relay Output
2 Volts/Line
1 Line/sec
Run 4 | 2nd Order System
Relay Input
0.2 Volts/Line
1 Line/sec
NO. RA 2921 30
BRUSH INSTRUMENTS
DIVISION OF CLEVITE CORPORATION
CLEVELAND, OHIO
PRINTED IN U.S.A.
Relay Output
2 Volts/Line
1 Line/sec

Figure 4.21. Typical Brush recordings of ramp responses.

graphically by plotting $\alpha_2 - \beta_2 = \alpha_1 - \beta_1$ vs. W for constant values of X. The value of W can then be obtained for any combination of $\frac{B\pi}{YK_{v_2}}$ and X. This information can in turn be used to calculate describing function curves which will be valid for two-sided operation. Unfortunately, this method is not easily adapted to a non-dimensionalized form. Consequently it must normally be calculated individually for each relay to be investigated.

The solution is slightly less complicated for a relay without hysteresis. The transfer characteristics for such a relay are shown in figure 3.1. In this case, $\alpha_1 = \beta_1$ and $\alpha_2 = \beta_2$. Therefore the system of simultaneous equations which must be solved in order to evaluate W consists of only equation 4.23 and equations I-9 and I-11.

$$4.23 \quad \beta_2 - \beta_1 = \frac{B\pi}{YK_{v_2}}$$

The equations for the coefficients of the fundamental components of the fourier series expansion of O(t) reduce to

$$4.24 \quad a_1 = 0$$

$$4.25 \quad b_1 = \frac{4Y}{\pi}(\cos\beta_1 + \cos\beta_2)$$

The solution can be simplified further by noting that

$$4.26 \quad \cos\beta_1 + \cos\beta_2 = 2\cos\tfrac{1}{2}(\beta_1 + \beta_2)\cos\tfrac{1}{2}(\beta_1 - \beta_2)$$

$$= 2\cos\tfrac{1}{2}(\beta_1 + \beta_2)\cos\frac{B\pi}{2YK_{v_2}}$$

$$4.27 \quad b_1 = \frac{4Y}{\pi}\cos\tfrac{1}{2}(\beta_1 + \beta_2)\cos\frac{B\pi}{2YK_{v_2}}$$

An even simpler solution can be obtained for a system containing an ideal relay. In this case there is no dead zone, and $\beta_1 = -\beta_2$. Therefore equation 4.27 reduces to equation 4.28 and the describing function can be expressed by equation 4.29.

$$4.28 \qquad b_1 = \frac{4Y}{\pi} \cos \frac{B\pi}{2K_{v_2}}$$

$$4.29 \qquad G_d = \frac{4Y}{\pi X} \cos \frac{B\pi}{2K_{v_2}} \qquad \angle 0^\circ$$

It should be noted that there will be a discontinuity between the describing function for one-sided operation and the describing function for two-sided operation whenever there is a significant hysteresis effect. Therefore, if the system is operating on only one side, and a small change in input or gain causes the error signal to change so that $X \geq X_c$, the system output may change radically.

It is possible that this discontinuity may help to predict some types of "jump resonance" found in relay servos. Suppose, for instance, that the system is subjected to a sinusoidal input, $\theta_i = A\sin \omega_o t$, such that $A\omega_o t = .9K_{v_2}$. If ω_o is much less than the natural frequencies of the system, the servo will behave as if the input signal were a slowly changing ramp which has a maximum slope of $A\omega_o$ at $\omega_o t = 0$ and decreases to zero at $\omega_o t = \frac{\pi}{2}$.

Now suppose the system characteristics are such that the relay will operate on only one side when $\omega_o t = 0$. Then the initial operating point will be determined by the ramp describing function for one-sided operation. The operating point will tend to travel along the linear curve, with the instantaneous operating point being determined by setting $B = A\omega_o \cos \omega_o t$.

If the linear curve crosses the critical curve of D_h for the relay used, the operating point will eventually reach a point where one-sided operation can no longer occur, and a two-sided limit cycle will result. During the next portion of the cycle, the servo will operate in accordance with the describing function for two-sided operation. The servo will return to one-sided operation when X decreases so that $D_n \geq \frac{X}{p_n - d_n}(1 + \sin\alpha_n)$, where both X and α_n are determined by the two-sided describing function.

In general, the magnitude of the system output will "jump" to a larger value when the relay shifts from one-sided operation to two-sided operation, and will "jump" to a smaller value whenever the relay returns to one-sided operation, due to the discontinuity between the two describing functions. There may also be a change in the frequency of the limit cycle when the shift occurs. Both the frequency change and magnitude change can easily be predicted once the describing function curves have been plotted.

4.6 Extension of the Ramp Describing Function to Other Types of Non-linearities.

The ramp describing function can be extended to apply to other types of non-linearities. In general, the fourier series expansion of the output wave will give several equations of the following types:

1. A relationship for a_0 similar to equation I-3.
2. Relationships for a_1 and b_1 similar to equations I-5 and I-7.
3. Relationships for all angles involved, similar to equations I-8 through I-11.

Since equation 2.20 applies for any non-linearity, it can be combined with the fourier equivalent of a_o to get a relation between the ramp magnitude and the angles involved, similar to equation 4.4. This in turn can be combined with the angle relationships to solve for the d.c. component, W. Once W is evaluated, it is a relatively simple matter to evaluate the equations for a_1 and b_1 and substitute these values into equation 3.8 to obtain the describing function.

It should be noted, however, that the transcendental equations involved will become more complex as the nature of the non-linearity becomes more complex, and the solution of these equations may become extremely difficult. In addition, other types of non-linearities may have different modes of operation corresponding to the one-sided and two-sided modes of operation for the relay servomechanism, and there may be discontinuities between the describing functions for these different modes.

Thus a complete analysis will require the evaluation of a separate group of describing function curves for each mode of operation, along with a set of limit curves to define the points at which the system will shift from one mode of operation to another.

CHAPTER V

RECOMMENDATIONS FOR FUTURE INVESTIGATIONS

During the course of this investigation, several interesting problems were noted which appeared to be worthy of further study. These suggested subjects are:

1. A comprehensive study of the effect of different types of dissymmetry on systems containing different types of non-linearities.
2. A more exhaustive analysis of the ramp describing function for a relay servomechanism in which the relay operates on both sides. This analysis should include an investigation of the discontinuity between the describing function for one-sided operation and the describing function for two-sided operation to determine whether or not these describing functions can be used to predict certain types of "jump resonance" effects, as suggested in section 4.5.
3. A thorough study of the extension of the ramp describing function to non-linear devices other than the relay would also be valuable to determine the effect of ramp inputs on systems containing such elements. An outline for the procedure for such an investigation is given in section 4.6.

BIBLIOGRAPHY

1. Kochenburger, R. J. Analysis and Synthesis of Contactor Servomechanisms, MIT Servomechanisms Laboratory Report No. 16, September 1, 1949.

2. Thaler, G. J., and R. G. Brown. Analysis and Design of Feedback Control Systems, McGraw-Hill Book Company, Inc., New York, 1960.

3. Langkamer, R. P., and T. J. Higgins. Describing Function Analysis of a Type 1 Control System with an Asymmetrical Deadzone Nonlinearity, AIEE Great Lakes District Conference Paper, April, 1961.

4. Song, Hui S. Simulation Techniques for Basic Non-linearities in Servomechanisms, Master of Science Thesis, U. S. Naval Postgraduate School, Monterey, California, 1960.

APPENDIX I

DERIVATION OF THE GENERALIZED DESCRIBING FUNCTION FOR A DISSYMETRIC RELAY

A. Input vs. output characteristics.

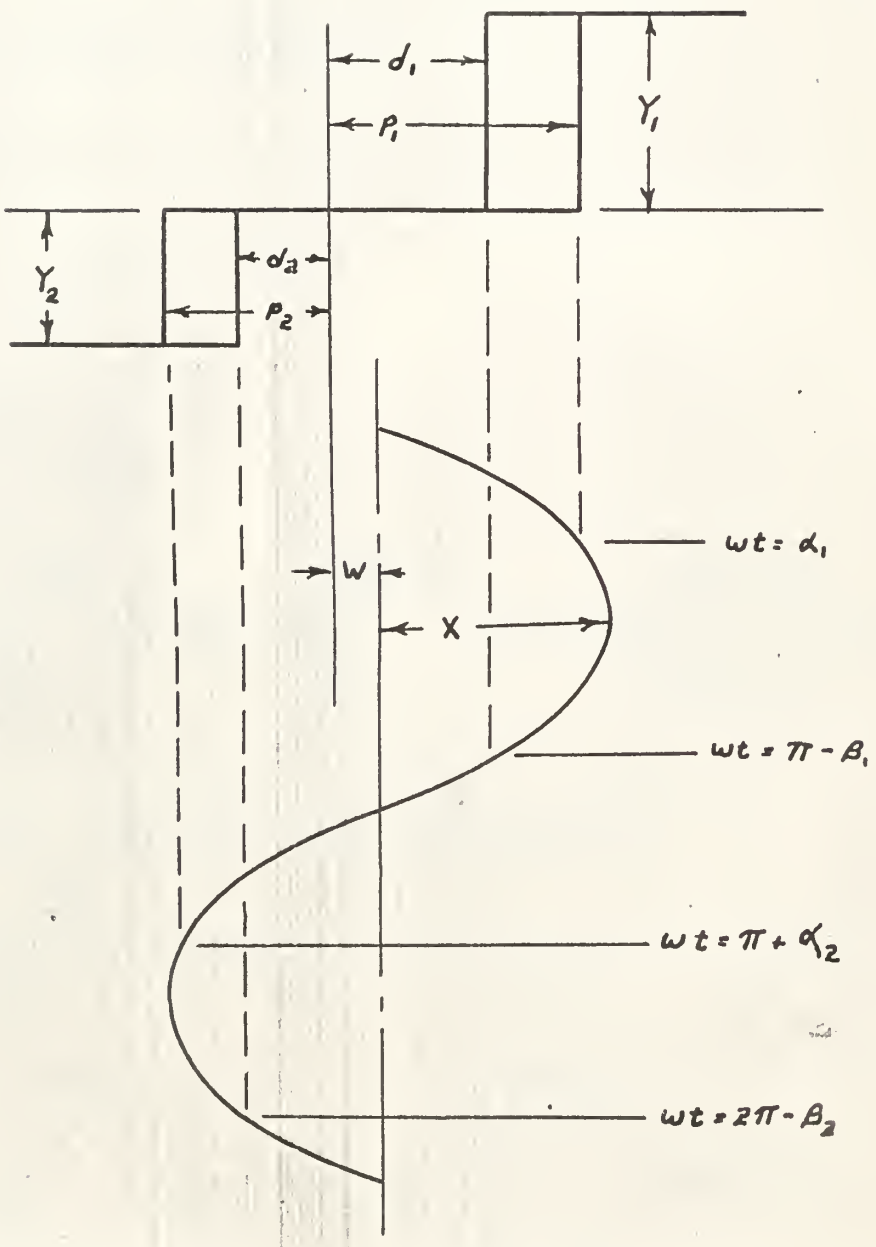

Figure I-1

2.1 $E(t) = E_m \sin \omega t$

I-1
$$O(t) = 0 \qquad 0 \le \omega t \le \alpha_1$$
$$O(t) = Y_1 \qquad \alpha_1 \le \omega t \le \pi - \beta_1$$
$$O(t) = 0 \qquad \pi - \beta_1 \le \omega t \le \pi + \alpha_2$$
$$O(t) = Y_2 \qquad \pi + \alpha_2 \le \omega t \le 2\pi - \beta_2$$
$$O(t) = 0 \qquad 2\pi - \beta_2 \le \omega t \le 2\pi$$

I. Fourier series expansion of output wave

2.2 $$O(t) = \frac{a_o}{2} + a_1 \cos \omega t + b_1 \sin \omega t$$

2.3 $$O(t) = \frac{a_o}{2} + C\sin(\omega t + \phi)$$

2.4 $$C = \sqrt{a_1^2 + b_1^2}$$

2.5 $$\phi = \tan^{-1} \frac{a_1}{b_1}$$

I-2
$$a_o = \frac{1}{\pi}\int_o^{2\pi} O(t)\, d\omega t = \frac{1}{\pi}\int_{\alpha_1}^{\pi-\beta_1} Y_1\, d\omega t + \frac{1}{\pi}\int_{\pi+\alpha_2}^{2\pi-\beta_2} Y_2\, d\omega t$$

I-3
$$a_o = \frac{1}{\pi}\left[Y_1(\pi - \beta_1 - \alpha_1) - Y_2(\pi - \beta_2 - \alpha_2)\right]$$

I-4
$$a_1 = \frac{1}{\pi}\int_o^{2\pi} O(t)\cos\omega t\, d\omega t$$
$$= \frac{1}{\pi}\int_{\alpha_1}^{\pi-\beta_1} Y_1\cos\omega t\, d\omega t + \frac{1}{\pi}\int_{\pi+\alpha_2}^{2\pi-\beta_2} -Y_2\cos\omega t\, d\omega t$$

I-5 $$a_1 = \frac{Y_1}{\pi}(\sin\beta_1 - \sin\alpha_1) + \frac{Y_2}{\pi}(\sin\beta_2 - \sin\alpha_2)$$

I-6 $$b_1 = \frac{1}{\pi}\int_0^{2\pi} G(\omega) \sin\omega t \, d\omega t$$

$$\frac{1}{\pi}\int_{\alpha_1}^{\pi-\beta_1} Y_1 \sin\omega t \, d\omega t + \frac{1}{\pi}\int_{\pi+\alpha_2}^{2\pi-\beta_2} Y_2 \sin\omega t \, d\omega t$$

I-7 $$b_1 = \frac{Y_1}{\pi}(\cos\alpha_1 + \cos\beta_1) + \frac{Y_2}{\pi}(\cos\alpha_2 + \cos\beta_2)$$

For a perfect sine input, the angles can be defined as follows:

I-8 $$\sin\alpha_1 = \frac{p_1 - W}{X} = R_{p_1}$$

I-9 $$\sin\beta_1 = \frac{d_1 - W}{X} = R_{d_1}$$

I-10 $$\sin\alpha_2 = \frac{p_2 - W}{X} = R_{p_2}$$

I-11 $$\sin\beta_2 = \frac{d_2 - W}{X} = R_{d_2}$$

C. The describing function.

The generalized describing function is:

3.8 $$G_d = \frac{1}{X}\sqrt{a_1^2 + b_1^2} \qquad \angle \tan^{-1}\frac{a_1}{b_1}$$

If both sides of the relay are actuated on each cycle, equations I-4 through I-7 can be used in the evaluation of equation 3.8 without restrictions. If the relay is only partially actuated, the same equations may still be used provided certain angles are defined as follows:

If $R_{p_n} \geq 1$, then $\alpha_n \triangleq \frac{\pi}{2}$ $\qquad n = 1,2$

If $R_{p_n} \leq -1$, then $\alpha_n = \frac{-\pi}{2}$ $\quad n = 1,2$

If $R_{d_n} \geq 1$, then $\beta_n = \frac{\pi}{2}$ $\quad n = 1,2$

If $R_{d_n} \geq -1$, then $\beta_n = \frac{-\pi}{2}$ $\quad n = 1,2$

D. Special Cases for $Y_1 = Y_2$

If $Y_1 = Y_2 = Y$, equations I-3, I-5, and I-7 reduce to

$$\text{I-12} \quad a_o = \frac{Y}{\pi}(\beta_2 + \alpha_2 - \beta_1 - \alpha_1)$$

$$\text{I-13} \quad a_1 = \frac{Y}{\pi}(\sin \beta_1 - \sin \alpha_1 + \sin \beta_2 - \sin \alpha_2)$$

$$\text{I-14} \quad b_1 = \frac{Y}{\pi}(\cos \beta_1 + \cos \alpha_1 + \cos \beta_2 + \cos \alpha_2)$$

If $Y_1 = Y_2 = Y$ and the relay has no hysteresis, then $\alpha_1 = \beta_1$, and $\alpha_2 = \beta_2$, and equations I-12, I-13 and I-14 reduce to

$$\text{I-15} \quad a_o = \frac{2Y}{\pi}(\beta_2 - \beta_1)$$

$$3.6 \quad a_1 = 0$$

$$\text{I-16} \quad b_1 = \frac{2Y}{\pi}(\cos \beta_2 + \cos \beta_1)$$

If $Y_1 = Y_2 = Y$ and the relay operates only on the positive side, then $\beta_2 \triangleq \alpha_2 \triangleq \frac{\pi}{2}$. The subscripts can be dropped for convenience in writing, so that equations I-12, I-13, and I-14 reduce to

$$4.1 \quad a_o = \frac{Y}{\pi}(\pi - \beta - \alpha)$$

$$4.2 \quad a_1 = \frac{Y}{\pi}(\sin \beta - \sin \alpha)$$

$$4.3 \quad b_1 = \frac{\pi}{\pi}(\cos \beta + \cos \alpha)$$

APPENDIX II

DERIVATION OF THE LIMIT OF SINUSOIDAL OPERATION DURING OPERATION ON ONLY ONE SIDE

When the relay operates on only one side, sinusoidal operation is possible only if $\alpha \leq 90°$.

$$4.4 \quad \frac{B}{EK_{V2}} = \frac{1}{2}(\pi - \beta - \alpha)$$

and

$$4.7 \quad \phi = \frac{\beta - \alpha}{2}$$

Therefore,

$$II\text{-}1 \quad \beta = \frac{\pi}{2} - \frac{B\pi}{EK_{V2}} + \phi$$

$$II\text{-}2 \quad \alpha = \frac{\pi}{2} - \frac{B\pi}{EK_{V2}} - \phi$$

For the case where $\beta < -\frac{\pi}{2}$, equation II-1 gives

$$II\text{-}3 \quad -\phi > \pi - \frac{B\pi}{EK_{V2}}$$

Therefore, if $B \geq .5EK_{V2}$, sinusoidal operation is possible only if

$$4.20 \quad -\phi \leq \pi - \frac{B\pi}{EK_{V2}}$$

For the case where $\alpha > \frac{\pi}{2}$, equation II-2 reduces to

$$II\text{-}5 \quad -\phi > \frac{B\pi}{EK_{V2}}$$

Therefore if $B \leq .5EK_{V2}$, sinusoidal operation is possible only if

$$4.21 \quad -\phi \leq \frac{B\pi}{EK_{V2}}$$